

Octahedral developing of knot complement II: Ptolemy coordinates and applications

Hyuk Kim

Department of Mathematical Sciences, Seoul National University, Seoul, 08826, Korea

Seonhwa Kim

School of Mathematics, Korea Institute for Advanced Study, Seoul 02455, Korea

Seokbeom Yoon

School of Mathematics, Korea Institute for Advanced Study, Seoul 02455, Korea

Abstract

It is known that a knot complement (minus two points) decomposes into ideal octahedra with respect to a given knot diagram. In this paper, we study the Ptolemy variety for such an octahedral decomposition in perspective of Thurston's gluing equation variety. More precisely, we compute explicit Ptolemy coordinates in terms of segment and region variables, the coordinates of the gluing equation variety motivated from the volume conjecture. As a consequence, we present an explicit formula for computing the obstruction to lifting a $(\mathrm{PSL}(2, \mathbb{C}), P)$ -representation of the knot group to a $(\mathrm{SL}(2, \mathbb{C}), P)$ -representation. We also present a diagrammatic algorithm to compute a holonomy representation of the knot group.

Keywords: Knots, diagrams, octahedral decompositions, Ptolemy coordinates.

2010 MSC: 57M25, 57M27, 55S35

1. Introduction

1.1. The gluing equation variety and Ptolemy variety

For a non-compact 3-manifold M with an ideal triangulation \mathcal{T} , the gluing equations are a system of algebraic equations consisting of an *edge equation* for each 1-cell of \mathcal{T} and some *cuspidal equations*. Letting $z_j \in \mathbb{C} \setminus \{0, 1\}$ ($1 \leq j \leq n$) be the shape parameters of the ideal tetrahedra of \mathcal{T} , the gluing equations are given by

$$\prod_{j=1}^n z_j^{A_{ij}} (1 - z_j)^{B_{ij}} = \pm 1$$

Email addresses: hyukkim@snu.ac.kr (Hyuk Kim), seonhwa17kim@kias.re.kr (Seonhwa Kim), sbyoon15@kias.re.kr (Seokbeom Yoon)

Preprint

March 2, 2022

for some integral matrices A and B (called the Neumann-Zagier matrices). We refer to [17] and [13] for details. The *gluing equation variety* $V(\mathcal{J})$ is an algebraic set in $(\mathbb{C} \setminus \{0, 1\})^n$ defined by the gluing equations. It is known that each point of $V(\mathcal{J})$ induces a $(\mathrm{PSL}(2, \mathbb{C}), P)$ -representation of $\pi_1(M)$ (or a boundary parabolic representation; see Definition 2.1) through the construction of so-called a pseudo-developing map (see, for instance, [14], [10]). We call the induced representation a *holonomy representation*. This allows us to think of $V(\mathcal{J})$ as a parameterization of $(\mathrm{PSL}(2, \mathbb{C}), P)$ -representations:

$$V(\mathcal{J}) \rightarrow \left\{ \begin{array}{c} (\mathrm{PSL}(2, \mathbb{C}), P)\text{-representations} \\ \pi_1(M) \rightarrow \mathrm{PSL}(2, \mathbb{C}) \end{array} \right\} / \text{Conjugation}.$$

A $(\mathrm{PSL}(2, \mathbb{C}), P)$ -representation may or may not be lifted to $\mathrm{SL}(2, \mathbb{C})$. Also, it may be lifted to an $\mathrm{SL}(2, \mathbb{C})$ -representation that is not $(\mathrm{SL}(2, \mathbb{C}), P)$ (or boundary unipotent). By the *obstruction class* of a $(\mathrm{PSL}(2, \mathbb{C}), P)$ -representation $\rho : \pi_1(M) \rightarrow \mathrm{PSL}(2, \mathbb{C})$ we mean the obstruction to lifting ρ to an $(\mathrm{SL}(2, \mathbb{C}), P)$ -representation. It is known that such an obstruction is a class in $H^2(\widehat{M}; \{\pm 1\})$ where \widehat{M} is the space obtained by adding a point to each ideal vertex of M (see [5, §2.1] for a brief review).

Inspired by the work of Fock-Goncharov [6], Garoufalidis-Thurston-Zickert [9] introduced the notion of Ptolemy variety for the ideal triangulation \mathcal{J} . The Ptolemy variety $P^\sigma(\mathcal{J})$ is defined for each 2-cocycle $\sigma \in Z^2(\widehat{M}; \{\pm 1\})$, but up to canonical isomorphism it only depends on the class $[\sigma] \in H^2(\widehat{M}; \{\pm 1\})$. Each point of $P^\sigma(\mathcal{J})$ is associated with a certain 1-cocycle on M (called a natural $(\mathrm{PSL}(2, \mathbb{C}), P)$ -cocycle; see Section 2) which induces a $(\mathrm{PSL}(2, \mathbb{C}), P)$ -representation with obstruction class $[\sigma]$. This gives us another parameterization of $(\mathrm{PSL}(2, \mathbb{C}), P)$ -representations:

$$P^\sigma(\mathcal{J}) \rightarrow \left\{ \begin{array}{c} (\mathrm{PSL}(2, \mathbb{C}), P)\text{-representations} \\ \pi_1(M) \rightarrow \mathrm{PSL}(2, \mathbb{C}) \\ \text{with obstruction class } [\sigma] \end{array} \right\} / \text{Conjugation}.$$

The way in which the Ptolemy variety produces $(\mathrm{PSL}(2, \mathbb{C}), P)$ -representations is more practical for computation, compared to the gluing equation variety, in the sense that there is no need to construct a pseudo-developing map. Also, there is a surjective map ψ defined tetrahedron-wise between these two varieties with the following commuting diagram (see Theorem 1.12 of [7]):

$$\begin{array}{ccc} \coprod_{[\sigma] \in H^2(\widehat{M}; \{\pm 1\})} P^\sigma(\mathcal{J}) & & \\ \psi \downarrow & \searrow & \\ V(\mathcal{J}) & \longrightarrow & \left\{ \begin{array}{c} (\mathrm{PSL}(2, \mathbb{C}), P)\text{-representations} \\ \pi_1(M) \rightarrow \mathrm{PSL}(2, \mathbb{C}) \end{array} \right\} / \text{Conjugation}. \end{array} \quad (1)$$

We note that there is an action T called the diagonal action on each $P^\sigma(\mathcal{J})$ (see [8]) so

that the map ψ factors through the action and induces a bijection $\bar{\psi}$:

$$\begin{array}{ccc}
\coprod_{[\sigma] \in H^2(\widehat{M}; \{\pm 1\})} P^\sigma(\mathcal{T})/T & & \\
\bar{\psi} \downarrow & \searrow & \\
V(\mathcal{T}) & \longrightarrow & \left\{ \begin{array}{l} (\mathrm{PSL}(2, \mathbb{C}), P)\text{-representations} \\ \pi_1(M) \rightarrow \mathrm{PSL}(2, \mathbb{C}) \end{array} \right\} / \text{Conjugation} .
\end{array} \tag{2}$$

1.2. Overview

For a knot $K \subset S^3$ it is known that the manifold $M = S^3 \setminus (K \cup \{p, q\})$ decomposes into ideal octahedra with respect to a given knot diagram, where $p \neq q \in S^3$ are two points not in K . We denote by \mathcal{T}_4 and \mathcal{T}_5 an ideal triangulation of M obtained by subdividing each ideal octahedron into ideal tetrahedra as in Figure 3 (left) and (right), respectively.

In the first paper [10] of the series, we have studied basic properties of \mathcal{T}_4 and \mathcal{T}_5 , mainly focused on pseudo-developing and holonomy via the gluing equations. The key point was that these ideal triangulations play a role of ‘‘canonical triangulation’’ with respect to a knot diagram and serve as a bridge between geometry of knot complement and combinatorics of knot diagram. In particular, we assign complex number z - (resp., w -) variables to the segments (resp., regions) of the knot diagram in order to parametrize the shapes of the ideal tetrahedra of \mathcal{T}_4 (resp., \mathcal{T}_5) (see Section 3 for a brief review). These variables were derived from the so-called optimistic limit of the Kashaev invariant and colored Jones polynomials in the volume conjecture (see [16], [19], [4], [3] for details, and see also [10] for geometric approach). In fact, those z - (resp., w -) variables correspond to the limiting indices in the summation of q -series expressions for the Kashaev invariant (resp., colored Jones polynomial).

Main aim of this paper is to construct an explicit section

$$\phi : V(\mathcal{T}) \rightarrow \coprod_{[\sigma] \in H^2(\widehat{M}; \{\pm 1\})} P^\sigma(\mathcal{T})$$

of the surjection ψ in the diagram (1) for $\mathcal{T} = \mathcal{T}_4$ and \mathcal{T}_5 (one may think of ϕ as the inverse of the bijection $\bar{\psi}$). More precisely, we shall compute explicit Ptolemy coordinates (the coordinates of the Ptolemy variety) in terms of z - and w -variables, respectively. The expression of Ptolemy coordinates given in the z - and w -variables turns out to be simple; for example, Ptolemy coordinates assigned to the side edges of an octahedron surprisingly turns out to be the same as w -variables of the corresponding regions, connecting hyperbolic geometry and quantum invariant in an unexpected way.

In general, contrast to ψ , a section ϕ can not be given tetrahedron-wise, since the construction of a pseudo-developing map is needed (see Section 2). However, it turns out that for the ideal triangulations \mathcal{T}_4 and \mathcal{T}_5 , it can be written ‘‘almost locally’’. That is, Ptolemy coordinates near a crossing are given by segment and region variables around the crossing with a single scaling parameter (see Section 3). This fact will be fruitfully used for our main formulas and their proofs.

As we mentioned earlier, Ptolemy coordinates efficiently produce $(\mathrm{PSL}(2, \mathbb{C}), P)$ -representations. Thus a holonomy representation $\rho : \pi_1(M) \rightarrow \mathrm{PSL}(2, \mathbb{C})$ can be directly computed in terms of z - and w -variables with the use of a section ϕ . As a consequence, we present diagrammatic formulas for computing

- the obstruction class of ρ (Theorem 4.1);
- the cusp shape of ρ (Theorem 5.1);
- the ρ -image of Wirtinger generators (Theorem 5.5).

On the other hand, the complex volume (volume and Chern-Simons invariant) of a $(\mathrm{PSL}(2, \mathbb{C}), P)$ -representation can be computed from Ptolemy coordinates. We refer to [9] and [21] for details. Thus a section ϕ also allows to compute the complex volume of a holonomy representation in terms of z - and w -variables. Such formulas, however, already presented by Cho-Murakami [4] and Cho-Kim-Kim [3] respectively. It is remarkable to notice that the formulas can be obtained without knowing all of exact Ptolemy coordinates. We will recall their formulas in this paper for convenience of the reader (Theorems 5.7 and 5.8).

For simplicity of exposition, we focus when K is a knot in S^3 . However, most of the discussions in this paper also work for a link in S^3 .

1.3. Organization

In Section 2, we recall how one constructs a section ϕ for a general 3-manifold. Precisely, we present how Ptolemy coordinates are computed from a pseudo-developing map. In Section 3, we present explicit Ptolemy coordinates for the ideal triangulations \mathcal{T}_4 and \mathcal{T}_5 in terms of z - and w -variables, respectively. A computation will be carried out by two steps. We first compute Ptolemy coordinates for each ideal octahedron and then glue them compatibly. In Sections 4 and 5, we prove the diagrammatic formulas that we mentioned earlier.

2. Ptolemy assignments from developing maps

2.1. Developing maps and decorations

Let M be a non-compact 3-manifold with an ideal triangulation \mathcal{T} . We denote by \widehat{M} the space obtained by adding a point to each ideal vertex of M , and denote by \overline{M} the compact manifold obtained by chopping off a small open regular neighborhood of each ideal vertex of M . The ideal triangulation of M endows \overline{M} with a decomposition into truncated tetrahedra whose triangular faces triangulate the boundary $\partial\overline{M}$. We call an edge of \overline{M} a *short-edge* if it is contained in $\partial\overline{M}$; a *long-edge*, otherwise (see Figure 1). Note that each long-edge of \overline{M} can be identified with an edge of M in an obvious way.

We denote by X^i the set of the oriented i -cells of X (unoriented when $i = 0$) for $X = \overline{M}, \partial\overline{M}, \widehat{M}$. For convenience reasons we let $M^i := \widehat{M}^i$. For instance, M^0 denotes the set of the ideal vertices of M . We shall use similar notations, such as $\overline{N}, \widehat{N}, N^i$, for the universal cover N of M where we denote the universal cover by N , instead of the usual notation \widetilde{M} , to avoid notational complexity.

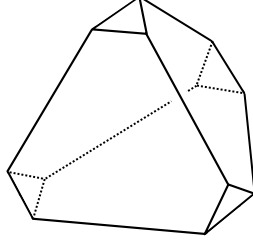


Figure 1: A truncated tetrahedron.

Definition 2.1. Let G be either $\mathrm{SL}(2, \mathbb{C})$ or $\mathrm{PSL}(2, \mathbb{C})$ and P be the subgroup of G consisting of upper triangular matrices with ones on the diagonal. A representation $\rho : \pi_1(M) = \pi_1(\bar{M}) \rightarrow G$ is called a (G, P) -representation if $\rho(\pi_1(\Sigma))$ lies up to conjugation in P for every component Σ of $\partial\bar{M}$.

Definition 2.2. For a (G, P) -representation $\rho : \pi_1(M) \rightarrow G$ a *(pseudo-)developing map* is a ρ -equivariant map $\mathcal{D} : \widehat{N} \rightarrow \overline{\mathbb{H}^3}$ such that $\mathcal{D}(N) \subset \mathbb{H}^3$ and $\mathcal{D}(N^0) \subset \partial\overline{\mathbb{H}^3}$, where ρ -equivariance means $\mathcal{D}(\gamma \cdot x) = \rho(\gamma)\mathcal{D}(x)$ for all $\gamma \in \pi_1(M)$ and $x \in \widehat{N}$.

Remark 2.3. If there is a loop γ in the link of $v \in N^0$ such that $\rho(\gamma) \neq I$, then the fact $\mathcal{D}(v) \in \partial\overline{\mathbb{H}^3}$ follows from ρ -equivariance and the fact that the subgroup P fixes a point only in $\partial\overline{\mathbb{H}^3}$.

It is well-known that any ρ -equivariant set map $N^0 \rightarrow \partial\overline{\mathbb{H}^3}$ extends to a developing map uniquely up to homotopy. This leads us to restrict our interest only on the ideal vertices.

Definition 2.4 ([21]). A *decoration* is a ρ -equivariant set map $\tilde{\mathcal{D}} : N^0 \rightarrow G/P$ where G/P denotes the left P -coset space.

Remark 2.5. The notion of a decoration contains additional geometric information (see [21, §3.1]), but it would not be considered in this paper.

For a P -coset gP we define $gP(\infty) := g'(\infty) \in \partial\overline{\mathbb{H}^3}$ for any coset representative g' of gP , regarding it as a Möbius transformation defined on $\mathbb{C} \cup \{\infty\} = \partial\overline{\mathbb{H}^3}$. Note that $gP(\infty)$ is well-defined as every element of P fixes ∞ .

Proposition 2.6. For a given developing map \mathcal{D} there exists a decoration $\tilde{\mathcal{D}}$ satisfying $(\tilde{\mathcal{D}}(v))(\infty) = \mathcal{D}(v)$ for all $v \in N^0$, i.e. the following diagram commutes:

$$\begin{array}{ccc}
 & & G/P \\
 & \nearrow \tilde{\mathcal{D}} & \downarrow \\
 N^0 & \xrightarrow{\mathcal{D}|_{N^0}} & \partial\overline{\mathbb{H}^3}
 \end{array}$$

where the vertical map is the evaluation by ∞ .

Proof. Let $V = \{v_1, \dots, v_h\} \subset N^0$ be the set of representatives of all the $\pi_1(M)$ -orbits in N^0 (so h is the number of the ideal vertices of M). For each $v_i \in V$ we let $\tilde{\mathcal{D}}(v_i) := g_i P$ for any $g_i \in G$ satisfying $g_i(\infty) = \mathcal{D}(v_i)$. For other $v \in N^0$ not in V we define $\tilde{\mathcal{D}}(v)$ ρ -equivariantly. Namely, we define $\tilde{\mathcal{D}}(v) := \rho(\gamma)\tilde{\mathcal{D}}(v_i) = \rho(\gamma)g_i P$ for $v_i \in V$ and $\gamma \in \pi_1(M)$ satisfying $v = \gamma \cdot v_i$. The choice of such $v_i \in V$ is unique but may not for a loop γ . We thus have to check well-definedness. Suppose that $v = \gamma \cdot v_i = \gamma' \cdot v_i$ for $\gamma, \gamma' \in \pi_1(M)$. Then $\rho(\gamma^{-1}\gamma')$ is a parabolic element fixing $g_i(\infty) = \mathcal{D}(v_i)$ and hence is an element of $g_i P g_i^{-1}$. Note that $g_i P g_i^{-1}$ is the set of all parabolic elements in G fixing $\mathcal{D}(v_i)$. It thus follows that $\rho(\gamma)g_i P = \rho(\gamma')g_i P$.

On the other hand, it is clear from construction that $(\tilde{\mathcal{D}}(v))(\infty) = \mathcal{D}(v)$ for all $v \in N^0$ \square

Remark 2.7. For each $v_i \in V$ there are \mathbb{C}^\times many scaling choices for $\tilde{\mathcal{D}}(v_i)$, so there are $(\mathbb{C}^\times)^h$ many choices for a decoration $\tilde{\mathcal{D}}$ in Proposition 2.6. This implies that the map ψ in the diagram (1) is $(\mathbb{C}^\times)^h$ -to-one (see Theorem 1.12 of [9]), since each decoration uniquely determines a point of the Ptolemy variety up to canonical isomorphism. However, as one can see in the diagram (2), such a scaling choice is inessential.

2.2. Ptolemy assignments

Let $\mathcal{D} : \widehat{N} \rightarrow \overline{\mathbb{H}^3}$ be a developing map for a (G, P) -representation $\rho : \pi_1(M) \rightarrow G$. Main aim of this section is to construct a Ptolemy assignment from a decoration given as in Proposition 2.6. We start with recalling the definition of Ptolemy varieties [9].

Definition 2.8. (a) The *Ptolemy variety* $P(\mathcal{J})$ is the set of all set maps $c : M^1 \rightarrow \mathbb{C}^\times$ satisfying $-c(e) = c(-e)$ for all $e \in M^1$ and

$$c(l_{02})c(l_{13}) = c(l_{03})c(l_{12}) + c(l_{01})c(l_{23}) \quad (3)$$

for each ideal tetrahedron Δ (with vertices $\{v_0, v_1, v_2, v_3\}$) of M , where l_{ij} is the oriented edge of Δ running from v_i to v_j (see Figure 2). Here $-e$ denotes the same edge e with the opposite orientation.

(b) For $\sigma \in Z^2(\widehat{M}; \{\pm 1\})$ the *Ptolemy variety* $P^\sigma(\mathcal{J})$ with the obstruction cocycle σ is the set of all set maps $c : M^1 \rightarrow \mathbb{C}^\times$ satisfying $-c(e) = c(-e)$ for all $e \in M^1$ and

$$\sigma_2 c(l_{02})c(l_{13}) = \sigma_3 c(l_{03})c(l_{12}) + \sigma_1 c(l_{01})c(l_{23}) \quad (4)$$

for each ideal tetrahedron Δ (with vertices $\{v_0, v_1, v_2, v_3\}$) of M , where σ_i is the σ -value on the face of Δ opposite to v_i . As the usual, $Z^2(\widehat{M}; \{\pm 1\})$ is the set of 2-cocycles of \widehat{M} with the coefficient $\{\pm 1\}$.

We call a point $c : M^1 \rightarrow \mathbb{C}^\times$ in either $P(\mathcal{J})$ or $P^\sigma(\mathcal{J})$ a *Ptolemy assignment*.

Let $\tilde{\mathcal{D}} : N^0 \rightarrow G/P$ be a decoration given as in Proposition 2.6. We consider a set map $\mathcal{C} : \overline{N}^0 \rightarrow G$ satisfying the following conditions:

- (i) $\mathcal{C}(x) \in \tilde{\mathcal{D}}(v)$ if $x \in \overline{N}^0$ is contained in the link of $v \in N^0$;
- (ii) $\mathcal{C}(x_0)^{-1}\mathcal{C}(x_1)$ is of the counter-diagonal form if x_0 and x_1 are joined by a long-edge of \overline{N} .

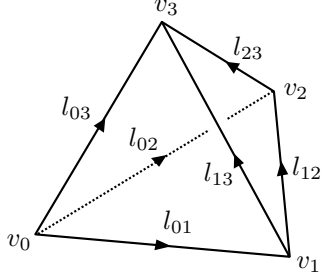


Figure 2: An ideal tetrahedron.

Under the assumption that every ideal tetrahedron of N has a non-degenerate image under the developing map \mathcal{D} , it is proved that such \mathcal{C} exists uniquely. See [21, Lemma 3.5]. Note that \mathcal{C} is also ρ -equivariant. We then define a set map $\mathcal{B} : \bar{N}^1 \rightarrow G$ by

$$\mathcal{B}(e) := \mathcal{C}(x_0)^{-1}\mathcal{C}(x_1) \quad (5)$$

for all $e \in \bar{N}^1$ where x_0 and x_1 are the initial and terminal vertices of e , respectively. Since we have

$$\begin{aligned} \mathcal{B}(\gamma \cdot e) &= \mathcal{C}(\gamma \cdot x_0)^{-1}\mathcal{C}(\gamma \cdot x_1) \\ &= (\rho(\gamma)\mathcal{C}(x_0))^{-1}\rho(\gamma)\mathcal{C}(x_1) \\ &= \mathcal{C}(x_0)^{-1}\mathcal{C}(x_1) = \mathcal{B}(e) \end{aligned}$$

for all $\gamma \in \pi_1(\bar{M})$ and $e \in \bar{N}^1$, it induces a set map $\mathcal{B} : \bar{M}^1 \rightarrow G$ (also denoted by \mathcal{B}). That is, for $e \in \bar{M}^1$ we define $\mathcal{B}(e) := \mathcal{B}(\tilde{e})$ where $\tilde{e} \in \bar{N}^1$ is any lifting of e .

The equation (5) implies that the set map \mathcal{B} is a cocycle: $\mathcal{B}(e)\mathcal{B}(-e) = I$ for all $e \in \bar{M}^1$ and $\mathcal{B}(e_1) \cdots \mathcal{B}(e_m) = I$ for each face $F \in \bar{M}^2$ where e_1, \dots, e_m are the boundary edges of F in order. We thus obtain an *induced* representation $\rho_0 : \pi_1(\bar{M}) \rightarrow G$ up to conjugation. Precisely, for $\gamma \in \pi_1(\bar{M})$, $\rho_0(\gamma)$ is given by the product of the \mathcal{B} -matrices along an edge-path of \bar{M} homotopic to γ . Note that well-definedness for ρ_0 follows from the cocycle condition of \mathcal{B} .

Proposition 2.9. The representation ρ_0 is conjugate to ρ , the one that we started with.

Proof. We fix a base point $x \in \bar{M}^0$ of $\pi_1(\bar{M})$ together with its lifting $\tilde{x} \in \bar{N}^0$. For a loop $\gamma \in \pi_1(\bar{M}, x)$ let γ_0 be an edge-path of \bar{M} based at x and homotopic to γ . Recall that $\rho_0(\gamma)$ is given by the product of the \mathcal{B} -matrices along γ_0 . Clearly, it is equal to the product of the \mathcal{B} -matrices along the lifting $\tilde{\gamma}_0$ of γ_0 . Here the lifting $\tilde{\gamma}_0$ is an edge-path of \bar{N} based at \tilde{x} . As $\tilde{\gamma}_0$ runs from \tilde{x} to $\gamma \cdot \tilde{x} (= \gamma_0 \cdot \tilde{x})$, the product along $\tilde{\gamma}_0$ results in $\mathcal{C}(\tilde{x})^{-1}\mathcal{C}(\gamma \cdot \tilde{x}) = \mathcal{C}(\tilde{x})^{-1}\rho(\gamma)\mathcal{C}(\tilde{x})$. It follows that $\rho_0(\gamma) = \mathcal{C}(\tilde{x})^{-1}\rho(\gamma)\mathcal{C}(\tilde{x})$ for all $\gamma \in \pi_1(\bar{M}, x)$. \square

The cocycle $\mathcal{B} : \bar{M}^1 \rightarrow G$ is called a *natural (G, P) -cocycle* in [7], [8] (or sometimes just a *natural cocycle*) since it only takes matrices of particular forms. Indeed, $\mathcal{B}(e) \in P$ for all short-edges e of \bar{M} and $\mathcal{B}(e)$ is of the counter-diagonal form for all long-edges e of \bar{M} . Note that this follows from the conditions (i) and (ii).

When $G = \mathrm{SL}(2, \mathbb{C})$, the natural cocycle \mathcal{B} can be encoded by a set map $c : \overline{M}^1 \rightarrow \mathbb{C}$ satisfying

$$\begin{cases} \mathcal{B}(e) = \begin{pmatrix} 0 & -c(e)^{-1} \\ c(e) & 0 \end{pmatrix} \text{ for all long-edges } e \in \overline{M}^1 \\ \mathcal{B}(e) = \begin{pmatrix} 1 & c(e) \\ 0 & 1 \end{pmatrix} \text{ for all short-edges } e \in \overline{M}^1. \end{cases} \quad (6)$$

We call $c(e)$ a *short-edge parameter* or a *long-edge parameter* according to an edge e . It is proved that long-edge parameters determine every short-edge parameter uniquely (see [21, Lemma 3.3]). Forgetting all short-edge parameters and identifying each long-edge of \overline{M} with an edge of M in an obvious way, we obtain a set map $c : M^1 \rightarrow \mathbb{C}^\times$ (also denoted by c).

Remark 2.10. The set map $c : M^1 \rightarrow \mathbb{C}^\times$ is directly computed from the decoration $\tilde{\mathcal{D}}$ as follows (see [21, Lemma 3.5]):

$$c(e) = \det \left(\tilde{\mathcal{D}}(v_0) \begin{pmatrix} 1 \\ 0 \end{pmatrix}, \tilde{\mathcal{D}}(v_1) \begin{pmatrix} 1 \\ 0 \end{pmatrix} \right) \quad (7)$$

for $e \in M^1$, where v_0 and v_1 are the initial and terminal ideal vertices of a lifting of e respectively. The determinant in the equation (7) does not depend on the choice of a lifting of e , since $\tilde{\mathcal{D}}$ is ρ -equivariant. Here $gP \begin{pmatrix} 1 \\ 0 \end{pmatrix} := g' \begin{pmatrix} 1 \\ 0 \end{pmatrix} \in \mathbb{C}^2$ for any coset representative g' of a P -coset gP .

Remark 2.11. The map $gP \mapsto gP \begin{pmatrix} 1 \\ 0 \end{pmatrix}$ gives an one-to-one correspondence between G/P and the non-zero vectors in \mathbb{C}^2 (up to sign when $G = \mathrm{PSL}(2, \mathbb{C})$).

Proposition 2.12. The set map $c : M^1 \rightarrow \mathbb{C}^\times$ is a point of the Ptolemy variety $P(\mathcal{J})$.

Proof. Due to the equation (7), it is clear that $-c(e) = c(-e)$ for all $e \in M^1$. For an ideal tetrahedron of M as in Figure 2 we let $V_i := \tilde{\mathcal{D}}(v_i) \begin{pmatrix} 1 \\ 0 \end{pmatrix}$ for $0 \leq i \leq 3$. Then the equation (7) also says that the equation (3) is equivalent to the Plücker relation

$$\det(V_0, V_2)\det(V_1, V_3) = \det(V_0, V_3)\det(V_1, V_2) + \det(V_0, V_1)\det(V_2, V_3).$$

□

When $G = \mathrm{PSL}(2, \mathbb{C})$, the short-edge parameters and long-edge parameters are similarly defined by using the equation (6). However, long-edge parameters shall have sign-ambiguity, since the counter-diagonal matrix in the equation (6) gives the same $\mathrm{PSL}(2, \mathbb{C})$ -matrix for both $c(e)$ and $-c(e)$. We therefore need to choose a sign for each long-edge parameter in order to define a set map $c : M^1 \rightarrow \mathbb{C}^\times$. Such a set map c may not be a point of $P(\mathcal{J})$ but is a point of $P^\sigma(\mathcal{J})$ for some $\sigma \in Z^2(\widehat{M}; \{\pm 1\})$.

Proposition 2.13. The set map $c : M^1 \rightarrow \mathbb{C}^\times$ is a point of the Ptolemy variety $P^\sigma(\mathcal{J})$ for some $\sigma \in Z^2(\widehat{M}; \{\pm 1\})$ whose class $[\sigma] \in H^2(\widehat{M}; \{\pm 1\})$ agrees with the obstruction class of the $(\mathrm{PSL}(2, \mathbb{C}), P)$ -representation $\rho : \pi_1(M) \rightarrow \mathrm{PSL}(2, \mathbb{C})$.

Proof. Recall that we have a natural $(\mathrm{PSL}(2, \mathbb{C}), P)$ -cocycle \mathcal{B} . The set map c uniquely determines a lifting $\tilde{\mathcal{B}} : \overline{M}^1 \rightarrow \mathrm{SL}(2, \mathbb{C})$ of \mathcal{B} such that $\tilde{\mathcal{B}}(e) \in P$ for all short-edges e of \overline{M} .

Clearly, $\tilde{\mathcal{B}}$ may not be a cocycle; the product of $\tilde{\mathcal{B}}$ -matrices along the boundary of each hexagonal face of \overline{M} is either I or $-I$. It thus induces a 2-cocycle $\sigma \in Z^2(\overline{M}, \partial\overline{M}; \{\pm 1\})$ whose class $[\sigma] \in H^2(\overline{M}, \partial\overline{M}; \{\pm 1\})$ is by definition the obstruction class of ρ .

We now consider an ideal tetrahedron Δ (with vertices $\{v_0, v_1, v_2, v_3\}$) of M with its truncation $\overline{\Delta}$. We denote by l_{ij} the long-edge of $\overline{\Delta}$ running from v_i to v_j , and denote by s_{jk}^i the short-edge of $\overline{\Delta}$ running from l_{ij} to l_{ik} . For notational simplicity we abbreviate $\tilde{\mathcal{B}}(l_{ij})$ and $\tilde{\mathcal{B}}(s_{jk}^i)$ by $\tilde{\mathcal{B}}_{ij}$ and $\tilde{\mathcal{B}}_{jk}^i \in P$, respectively.

Let $V_1 := \tilde{\mathcal{B}}_{01} \begin{pmatrix} 1 \\ 0 \end{pmatrix}$ and $V_i := \tilde{\mathcal{B}}_{1i}^0 \tilde{\mathcal{B}}_{0i} \begin{pmatrix} 1 \\ 0 \end{pmatrix}$ for $i = 2, 3$. Since every $\tilde{\mathcal{B}}_{jk}^i \in P$ fixes $\begin{pmatrix} 1 \\ 0 \end{pmatrix}$, we have $\det \left(\begin{pmatrix} 1 \\ 0 \end{pmatrix}, V_i \right) = c(l_{0i})$ for $1 \leq i \leq 3$. On the other hand, we have

$$\begin{aligned} \det(V_1, V_2) &= \det \left(\tilde{\mathcal{B}}_{01} \begin{pmatrix} 1 \\ 0 \end{pmatrix}, \tilde{\mathcal{B}}_{12}^0 \tilde{\mathcal{B}}_{02} \begin{pmatrix} 1 \\ 0 \end{pmatrix} \right) \\ &= \det \left(\tilde{\mathcal{B}}_{01} \begin{pmatrix} 1 \\ 0 \end{pmatrix}, \sigma_3 \tilde{\mathcal{B}}_{01} \tilde{\mathcal{B}}_{02}^1 \tilde{\mathcal{B}}_{12} \tilde{\mathcal{B}}_{10}^2 \begin{pmatrix} 1 \\ 0 \end{pmatrix} \right) \\ &= \sigma_3 \det \left(\begin{pmatrix} 1 \\ 0 \end{pmatrix}, \tilde{\mathcal{B}}_{02}^1 \tilde{\mathcal{B}}_{12} \begin{pmatrix} 1 \\ 0 \end{pmatrix} \right) \\ &= \sigma_3 c(l_{12}). \end{aligned}$$

where σ_i is the σ -value on the hexagonal face of $\overline{\Delta}$ opposite to v_i . For the second equality we use the definition of σ : $\tilde{\mathcal{B}}_{01} \tilde{\mathcal{B}}_{02}^1 \tilde{\mathcal{B}}_{12} \tilde{\mathcal{B}}_{10}^2 \tilde{\mathcal{B}}_{20} \tilde{\mathcal{B}}_{21}^0 = \sigma_3 I$. A similar computation shows that the Plücker relation for $V_0 := \begin{pmatrix} 1 \\ 0 \end{pmatrix}, V_1, V_2, V_3$ is equivalent to the equation (4):

$$\begin{aligned} \det(V_0, V_2) \det(V_1, V_3) &= \det(V_0, V_3) \det(V_1, V_2) + \det(V_0, V_1) \det(V_2, V_3) \\ \Leftrightarrow c(l_{02}) \sigma_2 c(l_{13}) &= c(l_{03}) \sigma_3 c(l_{12}) + c(l_{01}) \sigma_1 c(l_{23}). \end{aligned}$$

□

Remark 2.14. If we change the sign-choices that we made to define the set map c , the cocycle $\sigma \in Z^2(\widehat{M}; \{\pm 1\})$ may change, but the class $[\sigma] \in H^2(\widehat{M}; \{\pm 1\})$ should be the same. Since two Ptolemy varieties $P^{\sigma_1}(\mathcal{T})$ and $P^{\sigma_2}(\mathcal{T})$ are canonically isomorphic when $[\sigma_1] = [\sigma_2]$, the sign-choices for c as well as the cocycle σ itself are inessential.

3. Ptolemy assignments for an octahedral decomposition

Let K be a knot in S^3 with a fixed diagram D . It is known that $M = S^3 \setminus (K \cup \{p, q\})$, where $p \neq q \in S^3$ are two points not in K , decomposes into ideal octahedra (one per a crossing). See, for instance, [16], [18], [10]. We enumerate these ideal octahedra of M placed at the crossings by o_1, \dots, o_n (so n is the number of crossings of D). We denote by \mathcal{T}_4 (resp., \mathcal{T}_5) an ideal triangulation of M obtained by subdividing each o_i into ideal tetrahedra as in Figure 3 (left) (resp., (right)). Figure 3 is taken from [10].

In our previous paper [10], we expressed the gluing equations of \mathcal{T}_4 with the use of *segment variables* (denoted by z_i 's). As the name suggests, they are non-zero complex variables assigned to the segments of D . Here a segment is an edge of the diagram D viewing it as a 4-valent graph. Precisely, the gluing equations of \mathcal{T}_4 consist of the equation

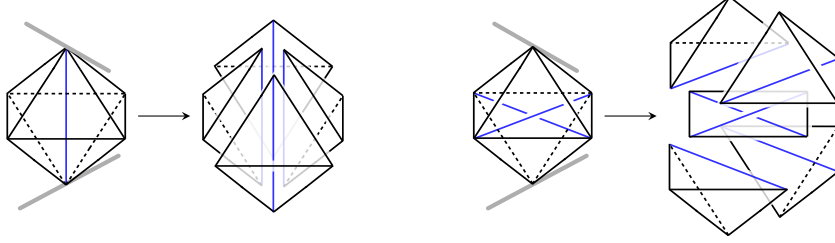


Figure 3: Subdivisions of an ideal octahedron.

(8) for each segment of D .

$$\left\{ \begin{array}{l} \frac{z_c - z_a}{z_c - z_b} \cdot \frac{z_d(z_c - z_e)}{z_e(z_c - z_d)} = 1 \text{ for Figure 4 (a)} \\ \frac{z_a(z_c - z_b)}{z_b(z_c - z_a)} \cdot \frac{z_c - z_d}{z_c - z_e} = 1 \text{ for Figure 4 (b)} \\ \frac{z_c - z_a}{z_c - z_b} \cdot \frac{z_c - z_e}{z_c - z_d} = 1 \text{ for Figure 4 (c)} \\ \frac{z_a(z_c - z_b)}{z_b(z_c - z_a)} \cdot \frac{z_e(z_c - z_d)}{z_d(z_c - z_e)} = 1 \text{ for Figure 4 (d)} \end{array} \right. \quad (8)$$

We always assume that two segment variables have distinct values if they (corresponding segments) share a crossing in D . For instance, we assume $z_a \neq z_c$, $z_b \neq z_c$, $z_d \neq z_c$, and $z_e \neq z_c$ for Figure 4. This assumption ensures that every ideal tetrahedron of \mathcal{T}_4 has non-degenerate shape (and also that terms in the equation (8) are well-defined). We refer to [10, §4.2] for details.

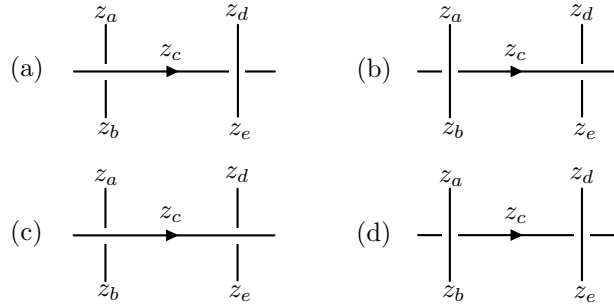


Figure 4: Segment variables around a segment.

Similarly, the gluing equations of \mathcal{T}_5 consist of a polynomial equation in *region variables* (denoted by w_i 's) for each region of D . The polynomial equation for a region, say R , is given by

$$\tau(\kappa_1) \cdots \tau(\kappa_m) = 1 \quad (9)$$

where $\kappa_1, \dots, \kappa_m$ denote the corners of R (so the region R is a m -gon) and the τ -value

of a corner is given by the rule

$$\tau(\kappa_i) = \frac{w_a w_c - w_b w_d}{(w_a - w_d)(w_c - w_d)}, \quad \tau(\kappa_j) = \frac{(w_b - w_c)(w_d - w_c)}{w_b w_d - w_a w_c} \quad (10)$$

for Figure 5. Here the τ -value is the cross-ratio of the tetrahedron measured at the side-edge of the octahedron posed at the corner (see [10]).

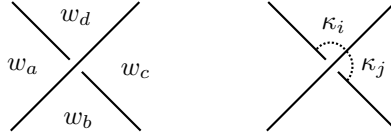


Figure 5: Region variables and corners around a crossing.

We always assume that the region variables have distinct values if they (corresponding regions) share a segment in D , and $w_a w_c \neq w_b w_d$ when region variables w_a, w_b, w_c, w_d gather around a crossing as in Figure 5 (left). This assumption ensures that every ideal tetrahedron of \mathcal{T}_5 has non-degenerate shape (and also that τ -values in the equation (10) are well-defined). We refer to [10, §4.3] for details.

3.1. Ptolemy assignments of \mathcal{T}_4

We fix a collection of segment variables z_i 's satisfying the gluing equations of \mathcal{T}_4 . We then obtain an associated developing map $\mathcal{D} : \widehat{N} \rightarrow \mathbb{H}^3$ together with a holonomy representation $\rho : \pi_1(M) \rightarrow \text{PSL}(2, \mathbb{C})$. Recall that N denotes the universal cover of M . For notational simplicity we shall identify an object in \widehat{N} with its image under \mathcal{D} . Main aim of this section is to compute a Ptolemy assignment for \mathcal{T}_4 in terms of the segment variables.

3.1.1. Ptolemy assignments on an ideal octahedron

We first consider an ideal octahedron o_i placed at a positive crossing. Recall that segment variables around the crossing give the coordinates of the ideal vertices of o_i where the bottom and top ideal vertices are fixed by 0 and $\infty \in \partial\overline{\mathbb{H}^3}$, respectively. See, for instance, Figures 6 (a) and 7 (left).

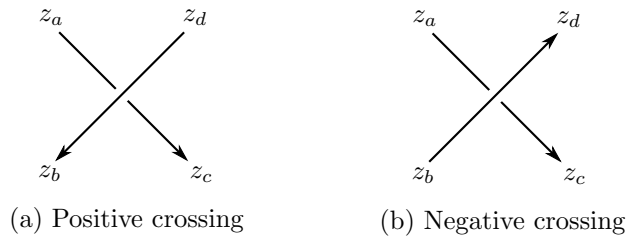


Figure 6: Segment variables around a crossing.

When we construct a developing map along the diagram, the octahedron o_i appears twice. We denote by O_i (resp., O^i) the one that appears when we over-pass (resp., under-pass) the crossing. We refer to [10, §4.1] for a detailed exposition. The coordinates of

the ideal vertices, denoted by $v_a, v_b, v_c, v_d, v_0, v_\infty$ as in Figure 7, of O_i are given by

$$\begin{cases} v_a = v_0 + \frac{z_a}{z_c - z_a}, & v_b = v_0 + \frac{z_b}{z_c - z_a}, \\ v_c = v_0 + \frac{z_c}{z_c - z_a}, & v_d = v_0 + \frac{z_d}{z_c - z_a}, & v_\infty = \infty. \end{cases} \quad (11)$$

Remark that O_i is normalized so that $v_c - v_a = 1$.

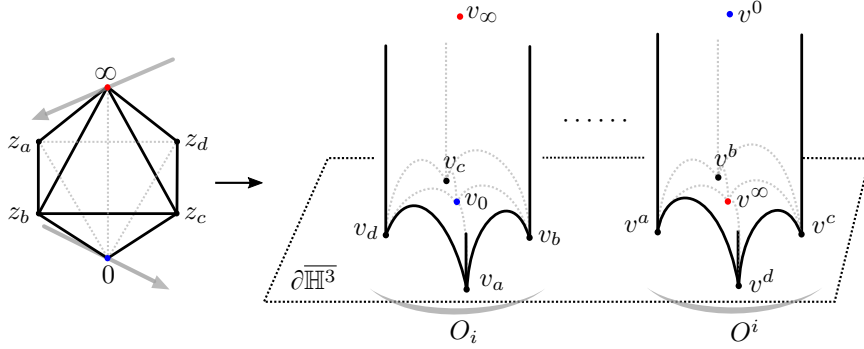


Figure 7: Two developing images O_i and O^i of o_i .

Let $\tilde{\mathcal{D}} : N^0 \rightarrow \text{PSL}(2, \mathbb{C})/P$ be a decoration given in Proposition 2.6. Recall that it satisfies $(\tilde{\mathcal{D}}(v_j))(\infty) = v_j$ for $j = a, b, c, d, 0, \infty$ respecting ρ -equivariance relation, where there are three equivariance relations on O_i since each ideal vertex of \mathcal{T}_4 appears in O_i twice. In [10] the authors showed that there exists a loop $\gamma_1 \in \pi_1(M)$ whose holonomy action $\rho(\gamma_1)$ is parabolic satisfying $\rho(\gamma_1) \cdot v_a = v_c$ and $\rho(\gamma_1) \cdot v_\infty = v_\infty$. Also, there exists $\gamma_2 \in \pi_1(M)$ whose holonomy action $\rho(\gamma_2)$ is parabolic satisfying $\rho(\gamma_2) \cdot v_d = v_b$ and $\rho(\gamma_2) \cdot v_0 = v_0$. In fact, the loop γ_1 (resp., γ_2) is a meridian winding an over-arc (resp., under-arc) of the crossing. See [10, Remark 5.11]. A straightforward computation using the equation (11) gives

$$\rho(\gamma_1) = \begin{pmatrix} 1 & 1 \\ 0 & 1 \end{pmatrix}, \quad \rho(\gamma_2) = \begin{pmatrix} 1 & v_0 \\ 0 & 1 \end{pmatrix} \begin{pmatrix} 1 & 0 \\ \Lambda & 1 \end{pmatrix} \begin{pmatrix} 1 & -v_0 \\ 0 & 1 \end{pmatrix}$$

where $\Lambda := (z_c - z_a)(\frac{1}{z_b} - \frac{1}{z_d})$. It thus follows that

$$\tilde{\mathcal{D}}(v_c) = \begin{pmatrix} 1 & 1 \\ 0 & 1 \end{pmatrix} \tilde{\mathcal{D}}(v_a), \quad \tilde{\mathcal{D}}(v_b) = \begin{pmatrix} 1 & v_0 \\ 0 & 1 \end{pmatrix} \begin{pmatrix} 1 & 0 \\ \Lambda & 1 \end{pmatrix} \begin{pmatrix} 1 & -v_0 \\ 0 & 1 \end{pmatrix} \tilde{\mathcal{D}}(v_d). \quad (12)$$

Remark 3.1. Since there is an edge of \mathcal{T}_4 joining the top and bottom vertices of o_i , we have $v_0 \neq v_\infty = \infty$ (for details see [14]). This may not be true for \mathcal{T}_5 . See Section 3.2.

On the other hand, there exists $\gamma_3 \in \pi_1(M)$ satisfying $O_i = \gamma_3 \cdot O^i$, since both O_i and O^i are liftings of o_i . The vertex v^0 of O^i corresponding to v_0 coincides with v_∞ in \widehat{N} (both v_∞ and v^0 are placed at ∞ as in Figure 7). In particular, we have $\tilde{\mathcal{D}}(v^0) = \tilde{\mathcal{D}}(v_\infty)$, so $\tilde{\mathcal{D}}(v_0) = \rho(\gamma_3)\tilde{\mathcal{D}}(v^0) = \rho(\gamma_3)\tilde{\mathcal{D}}(v_\infty)$. From the fact $O_i = \gamma_3 \cdot O^i$, one can compute

that

$$\tilde{\mathcal{D}}(v_0) = \begin{pmatrix} 1 & v_0 \\ 0 & 1 \end{pmatrix} \begin{pmatrix} 0 & \sqrt{-\Lambda^{-1}} \\ -\sqrt{-\Lambda} & 0 \end{pmatrix} \begin{pmatrix} 1 & -v^\infty \\ 0 & 1 \end{pmatrix} \tilde{\mathcal{D}}(v_\infty) \quad (13)$$

where v^∞ is the vertex of O^i corresponding to v_∞ .

Since $(\tilde{\mathcal{D}}(v_j))(\infty) = v_j$ for each v_j , $\tilde{\mathcal{D}}(v_j)$ is of the form $\begin{pmatrix} \alpha & * \\ \beta & * \end{pmatrix} P$ for some $\alpha, \beta \in \mathbb{C}$ satisfying $v_j = \frac{\alpha}{\beta} \in \mathbb{C} \cup \{\infty\}$. We let

$$\begin{cases} \tilde{\mathcal{D}}(v_a) = \frac{p_i}{\sqrt{z_c - z_a}} \begin{pmatrix} 1 & v_0 \\ 0 & 1 \end{pmatrix} \begin{pmatrix} z_a & * \\ z_c - z_a & * \end{pmatrix} P \\ \tilde{\mathcal{D}}(v_d) = p_i \sqrt{z_c - z_a} \begin{pmatrix} 1 & v_0 \\ 0 & 1 \end{pmatrix} \begin{pmatrix} \frac{1}{z_c - z_a} & * \\ \frac{1}{z_d} & * \end{pmatrix} P \\ \tilde{\mathcal{D}}(v_\infty) = \begin{pmatrix} 1 & v_0 \\ 0 & 1 \end{pmatrix} \begin{pmatrix} 1 & * \\ 0 & * \end{pmatrix} P \end{cases} \quad (14)$$

for some $p_i \in \mathbb{C} \setminus \{0\}$ so that ρ -equivariance relations (12) and (13) give

$$\begin{cases} \tilde{\mathcal{D}}(v_c) = \frac{p_i}{\sqrt{z_c - z_a}} \begin{pmatrix} 1 & v_0 \\ 0 & 1 \end{pmatrix} \begin{pmatrix} z_c & * \\ z_c - z_a & * \end{pmatrix} P \\ \tilde{\mathcal{D}}(v_b) = p_i \sqrt{z_c - z_a} \begin{pmatrix} 1 & v_0 \\ 0 & 1 \end{pmatrix} \begin{pmatrix} \frac{1}{z_c - z_a} & * \\ \frac{1}{z_b} & * \end{pmatrix} P \\ \tilde{\mathcal{D}}(v_0) = \begin{pmatrix} 1 & v_0 \\ 0 & 1 \end{pmatrix} \begin{pmatrix} 0 & * \\ -\sqrt{-\Lambda} & * \end{pmatrix} P \end{cases}$$

Remark 3.2. There are many other possible scaling choices for $\tilde{\mathcal{D}}$ (see Remark 2.7), but the choice given in the equation (14) is enough to construct a Ptolemy assignment on the whole manifold M . (see Section 3.1.2). Also, note that $\sqrt{z_c - z_a}$ in the decoration $\tilde{\mathcal{D}}$ in the equation (14) is designed so that the expression of the resulting Ptolemy assignment is in symmetry (see Figure 8 below).

Using the equation (7), one can compute a Ptolemy assignment on o_i as in Figure 8. Remark that the variable v_0 vanishes in Figure 8. A Ptolemy assignment for a negative crossing as in Figure 6 (b) is computed similarly. It results in the same as Figure 8 except that every term $\sqrt{z_c - z_a}$ should be replaced by $\sqrt{z_a - z_c}$.

Even though we started with a $(\mathrm{PSL}(2, \mathbb{C}), P)$ -representation ρ , the Ptolemy assignment given in Figure 8 satisfies the equation (3) for each ideal tetrahedron of o_i . It thus induces a natural $(\mathrm{SL}(2, \mathbb{C}), P)$ -cocycle $\mathcal{B}_i : \bar{o}_i^1 \rightarrow \mathrm{SL}(2, \mathbb{C})$ (recall that \bar{o}_i^1 denotes the set of the oriented 1-cells of a truncated octahedron \bar{o}_i of o_i). Using Lemma 3.3 in [21],

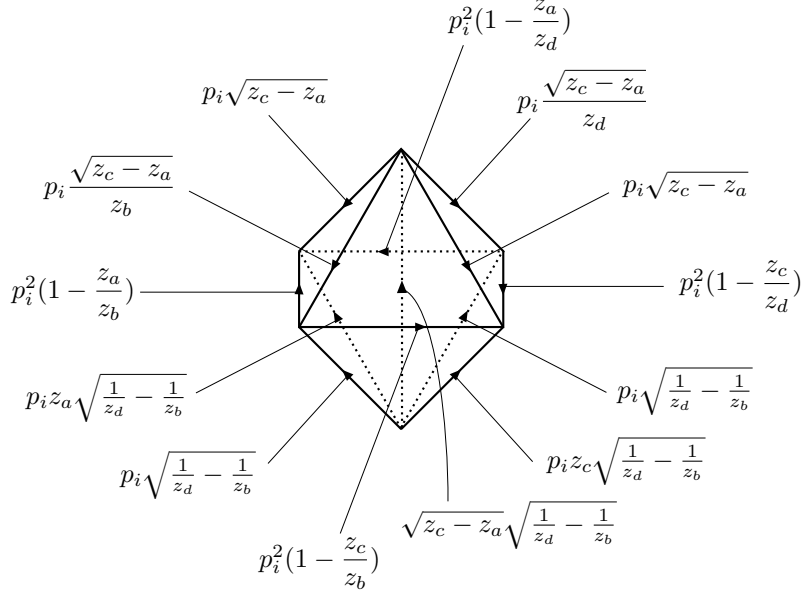


Figure 8: A Ptolemy assignment at a positive crossing.

short-edge parameters of \mathcal{B}_i for a positive crossing are computed as follows:

$$\begin{aligned}
\textcircled{a} &= \frac{z_a - z_d}{z_c - z_a} & \textcircled{b} &= \frac{z_b - z_a}{z_c - z_a} & \textcircled{c} &= \frac{z_c - z_b}{z_c - z_a} & \textcircled{d} &= \frac{z_d - z_c}{z_c - z_a} \\
\textcircled{e} &= \frac{z_b}{p_i^2 z_a (z_b - z_a)} & \textcircled{f} &= \frac{z_d}{p_i^2 z_a (z_a - z_d)} & \textcircled{g} &= \frac{1}{p_i^2 (z_d - z_a)} & \textcircled{h} &= \frac{1}{p_i^2 (z_a - z_b)} \\
\textcircled{i} &= \frac{z_a z_b}{p_i^2 (z_a - z_b)} & \textcircled{j} &= \frac{z_b z_c}{p_i^2 (z_b - z_c)} & \textcircled{k} &= \frac{z_b^2}{p_i^2 (z_c - z_b)} & \textcircled{l} &= \frac{z_b^2}{p_i^2 (z_b - z_a)} \\
\textcircled{m} &= \frac{z_d (z_c - z_b)}{z_c (z_b - z_d)} & \textcircled{n} &= \frac{z_b (z_d - z_c)}{z_c (z_b - z_d)} & \textcircled{o} &= \frac{z_b (z_a - z_d)}{z_a (z_b - z_d)} & \textcircled{p} &= \frac{z_d (z_b - z_a)}{z_a (z_b - z_d)} \\
\textcircled{q} &= \frac{z_b}{p_i^2 z_c (z_b - z_c)} & \textcircled{r} &= \frac{z_d}{p_i^2 z_c (z_c - z_d)} & \textcircled{s} &= \frac{1}{p_i^2 (z_d - z_c)} & \textcircled{t} &= \frac{1}{p_i^2 (z_c - z_b)} \\
\textcircled{u} &= \frac{z_a z_d}{p_i^2 (z_a - z_d)} & \textcircled{v} &= \frac{z_c z_d}{p_i^2 (z_d - z_c)} & \textcircled{w} &= \frac{z_d^2}{p_i^2 (z_c - z_d)} & \textcircled{x} &= \frac{z_d^2}{p_i^2 (z_d - z_a)}
\end{aligned} \tag{15}$$

for Figure 9. Note that not all short-edges are presented in Figure 9. Short-edge parameters of \mathcal{B}_i for a negative crossing are the same as those for a positive crossing except that the sign of $\textcircled{a}, \dots, \textcircled{d}$ should be changed.

3.1.2. Gluing the octahedra

As the ideal octahedra o_1, \dots, o_n glue their faces to form the manifold M , certain relations among the variables p_1, \dots, p_n are required to glue the natural cocycles \mathcal{B}_i 's compatibly. We refer to [10, §3.1] for the gluing-pattern of the ideal octahedra o_1, \dots, o_n .

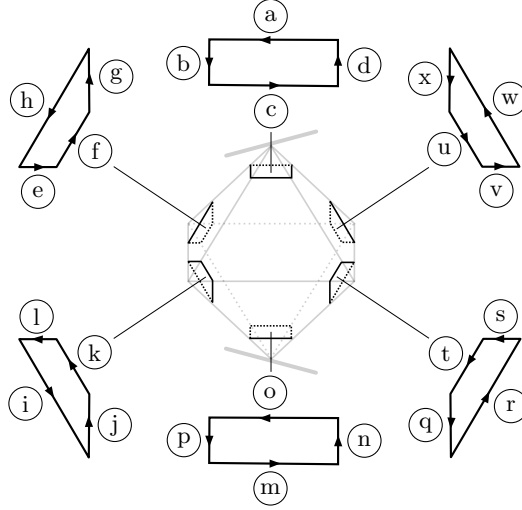


Figure 9: Short-edges of a truncated octahedron.

One can check that the relations among p_1, \dots, p_n consist of

$$\left\{ \begin{array}{l} p_i \sqrt{1 - \frac{z_b}{z_c}} = p_j \sqrt{1 - \frac{z_c}{z_e}} \text{ for Figure 4 (a)} \\ p_i \sqrt{1 - \frac{z_c}{z_b}} = p_j \sqrt{1 - \frac{z_e}{z_c}} \text{ for Figure 4 (b)} \\ p_i \sqrt{1 - \frac{z_b}{z_c}} = p_j \sqrt{1 - \frac{z_e}{z_c}} \text{ for Figure 4 (c)} \\ p_i \sqrt{1 - \frac{z_c}{z_b}} = p_j \sqrt{1 - \frac{z_c}{z_e}} \text{ for Figure 4 (d)} \end{array} \right. \quad (16)$$

for each segment of D , where i and j are the indices of ideal octahedra placed at the crossing in the left and right of the segment, respectively.

It turns out that it may not be possible to glue all \mathcal{B}_i 's compatibly (see Section 4). However, it is possible if we project them down to $\text{PSL}(2, \mathbb{C})$ (see Proposition 3.3 below). Since the cocycle \mathcal{B}_i represents the same natural $(\text{PSL}(2, \mathbb{C}), P)$ -cocycle for both p_i and $-p_i$, we may regard the variable p_i as an element of $\mathbb{C}^\times / \{\pm 1\}$.

Proposition 3.3. Regarding each p_i as an element of $\mathbb{C}^\times / \{\pm 1\}$, there exists a collection of p_1, \dots, p_n satisfying the equation (16) for every segment of D . Moreover, it is unique up to scaling.

Proof. It is clear that all p_i 's are successively determined by using the equation (16) whenever one of them is chosen arbitrarily. The uniqueness is obvious when we prove compatibility of such determinations. It suffices to check that such determinations are compatible when we do these along the boundary of each region, say R , of D .

Suppose that R is given as in Figure 10. Due to the equation (8), the equation (16)

for Figure 4 (a) is equivalent to

$$p_i \sqrt{1 - \frac{z_a}{z_c}} = p_j \sqrt{1 - \frac{z_c}{z_d}}$$

up to sign. Therefore, relations among p_1, \dots, p_m arising from the segments lying in the boundary of R consist of

$$p_i \sqrt{1 - \frac{z_i}{z_{i+1}}} = p_{i+1} \sqrt{1 - \frac{z_{i+1}}{z_{i+2}}}$$

up to sign for $1 \leq i \leq m$. Here the index is taken in modulo m . These relations are compatible as their cyclic product along the boundary results in the trivial one. We proved the case when the boundary of R is alternating as in Figure 10, but one can prove similarly for other cases. \square

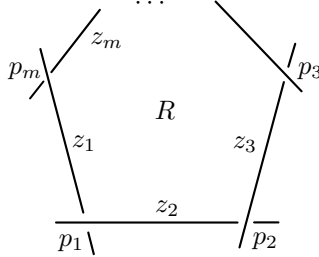


Figure 10: Segment variables around a region.

Remark 3.4. As we shall see in Section 5, exact values of the variables p_1, \dots, p_n are not that important. They will disappear in the computation for a holonomy representation (see also Section 3.1.3).

One can restate Proposition 3.3 as follows.

Corollary 3.5. The natural cocycles $\mathcal{B}_i : \bar{o}_i^1 \rightarrow \mathrm{PSL}(2, \mathbb{C})$ ($1 \leq i \leq n$) are well-glued so as to form a natural $(\mathrm{PSL}(2, \mathbb{C}), P)$ -cocycle $\mathcal{B} : \bar{M}^1 \rightarrow \mathrm{PSL}(2, \mathbb{C})$ on the manifold M .

In particular, we obtain a Ptolemy assignment $c : M^1 \rightarrow \mathbb{C}^\times$ after some sign-choices. Due to Proposition 2.13 such c is a point of $P^\sigma(\mathcal{T}_4)$ for some $\sigma \in Z^2(\widehat{M}; \{\pm 1\})$ whose class is the obstruction class of the holonomy representation ρ . We shall analyze this class in Section 4.

3.1.3. Simplification by a graph

The Ptolemy assignment of \mathcal{T}_4 (including the short-edge parameters) in the previous section seems somewhat complicated as there are too many edges. For its simplification we suggest a graph G in M as follows. This is motivated by the work of Thistlethwaite-Tsvietkova [15] (see also [12]).

1. Place a *vertical edge* at each crossing of D so that it represents the central axis of the ideal octahedron o_i (see Figure 11);

2. For each segment of D join the vertices of G by either one or two *horizontal edges* along the segment as in Figure 11.

Note that any loop in M can be represented by an edge-path of G ,

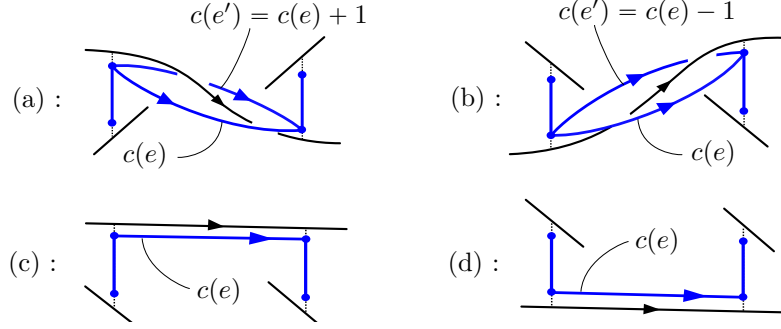


Figure 11: Local configuration of G for Figure 4

Each vertical edge of G is a long-edge of \bar{M} and each horizontal edge of G is the composition of two short-edges of \bar{M} . Therefore, a natural cocycle $\mathcal{B} : \bar{M}^1 \rightarrow \text{PSL}(2, \mathbb{C})$ in the previous section endows each edge of G with a *long-* or *short-edge parameter*, accordingly. Precisely, the long-edge parameter $c(e) \in \mathbb{C}^\times / \{\pm 1\}$ of a vertical edge e of G is given by

$$c(e) = \begin{cases} \sqrt{(z_a - z_c) \left(\frac{1}{z_d} - \frac{1}{z_b} \right)} & \text{for Figure 6(a)} \\ \sqrt{(z_a - z_c) \left(\frac{1}{z_b} - \frac{1}{z_d} \right)} & \text{for Figure 6(b)} \end{cases}$$

(cf. Figure 8) and the short-edge parameter $c(e) \in \mathbb{C}$ of a horizontal edge e of G is given by

$$c(e) = \begin{cases} \frac{z_c}{z_a - z_b} - \frac{z_d}{z_d - z_e} & \text{for Figure 11(a)} \\ \frac{z_a}{z_a - z_b} - \frac{z_c}{z_d - z_e} & \text{for Figure 11(b)} \\ \frac{z_c}{z_a - z_b} - \frac{z_c}{z_d - z_e} & \text{for Figure 11(c)} \\ \frac{z_a}{z_a - z_c} - \frac{z_d}{z_d - z_e} & \text{for Figure 11(d)} \end{cases}$$

Note that the variable p_i does not appear in the above equations.

Remark 3.6. In [12] (resp., [15]), such long-edge parameters of G are called intercus parameters (resp., crossing labels) and such short-edge parameters of G are called translation parameters (resp., edge labels).

3.2. Ptolemy assignments of \mathcal{T}_5

We fix a collection of region variables w_i 's satisfying the gluing equations of \mathcal{T}_5 and let $\rho : \pi_1(M) \rightarrow \text{PSL}(2, \mathbb{C})$ be the holonomy representation. In this section, we compute

a Ptolemy assignment of \mathcal{F}_5 in terms of region variables by using the same strategy that we used in Section 3.1. Computations in this section will be similar to those in Section 3.2, so some of them will be omitted.

3.2.1. Ptolemy assignments on an ideal octahedron

We first consider an ideal octahedron o_i placed at a positive crossing. We denote region variables around the crossing as in Figure 12 (a). Ratios of these variables give us the cross-ratios of the ideal tetrahedra of o_i (see [10, §4.3]). In particular, we have

$$[v_b, v_\infty, v_c, v_a] = \frac{w_a}{w_b}, [v_d, v_\infty, v_a, v_c] = \frac{w_c}{w_d}, [v_0, v_c, v_d, v_b] = \frac{w_c}{w_b} \quad (17)$$

for the ideal octahedron O_i with vertices $v_a, v_b, v_c, v_d, v_0, v_\infty$ as in Figure 7, where the notation $[x, y, z, w]$ means the cross-ratio $\frac{(x-w)(y-z)}{(x-z)(y-w)}$. Recall that the octahedron O_i is normalized so that $v_c - v_a = 1$ and $v_\infty = \infty$. We may further assume that $v_a = 0$ (so $v_c = 1$), since we already saw in Section 3.1 that only relative coordinates of the ideal vertices matter when we compute a Ptolemy assignment. A straightforward computation using the equation (17) gives

$$v_b = \frac{w_a}{w_a - w_b}, v_d = \frac{w_d}{w_d - w_c}, v_0 = \frac{w_a - w_d}{w_a - w_b + w_c - w_d}.$$

Remark that we allow the case $v_0 = \infty$, that is when $w_a - w_b + w_c - w_d = 0$.

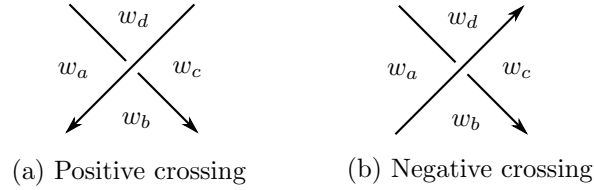


Figure 12: Region variables around a crossing.

We use the same loops $\gamma_1, \gamma_2, \gamma_3 \in \pi_1(M)$ in Section 3.1 to compute ρ -equivariance relations for a decoration $\tilde{\mathcal{D}}$. When $v_0 \neq \infty$, a computation will be exactly same as in Section 3.1, so the ρ -equivariance relations also result in the same as in the equations (12) and (13) except that Λ is now given by

$$\Lambda := \frac{(w_a - w_b + w_c - w_d)^2}{w_a w_c - w_b w_d}. \quad (18)$$

We can let

$$\tilde{\mathcal{D}}(v_a) = q_i \begin{pmatrix} 0 & * \\ 1 & * \end{pmatrix} P, \quad \tilde{\mathcal{D}}(v_d) = \frac{1}{q_i} \begin{pmatrix} w_d & * \\ w_d - w_c & * \end{pmatrix} P, \quad \tilde{\mathcal{D}}(v_\infty) = \begin{pmatrix} 1 & * \\ 0 & * \end{pmatrix} P \quad (19)$$

for some $q_i \in \mathbb{C} \setminus \{0\}$ so that equivariance relations (12) and (13) give

$$\tilde{\mathcal{D}}(v_c) = q_i \begin{pmatrix} 1 & * \\ 1 & * \end{pmatrix} P, \quad \tilde{\mathcal{D}}(v_b) = \frac{1}{q_i} \begin{pmatrix} w_a & * \\ w_a - w_b & * \end{pmatrix} P, \quad \tilde{\mathcal{D}}(v_0) = \sqrt{-\Lambda} \begin{pmatrix} v_0 & * \\ 1 & * \end{pmatrix} P.$$

Then using the equation (7), one can compute a Ptolemy assignment on the ideal octahedron o_i as in Figure 13. When $v_0 = \infty$ ($\Leftrightarrow w_a - w_b + w_c - w_d = 0$), a holonomy computation for γ_2 and γ_3 should be changed to

$$\rho(\gamma_2) = \begin{pmatrix} 1 & v_b - v_d \\ 0 & 1 \end{pmatrix}, \quad \rho(\gamma_3) = \begin{pmatrix} \frac{\sqrt{w_b w_d - w_a w_c}}{w_a - w_b} & \frac{-w_d}{\sqrt{w_b w_d - w_a w_c}} \\ 0 & \frac{w_a - w_b}{\sqrt{w_b w_d - w_a w_c}} \end{pmatrix}.$$

However, the decoration $\tilde{\mathcal{D}}$ chosen as in the equation (19) still gives the same Ptolemy assignment as in Figure 13. We note that the following identity is used:

$$w_b w_d - w_a w_c = w_b w_d - w_a w_c + w_a(w_a - w_b + w_c - w_d) = (w_a - w_b)(w_a - w_d).$$

A Ptolemy assignment for a negative crossing as in Figure 12 (b) is computed similarly. See Figure 14.

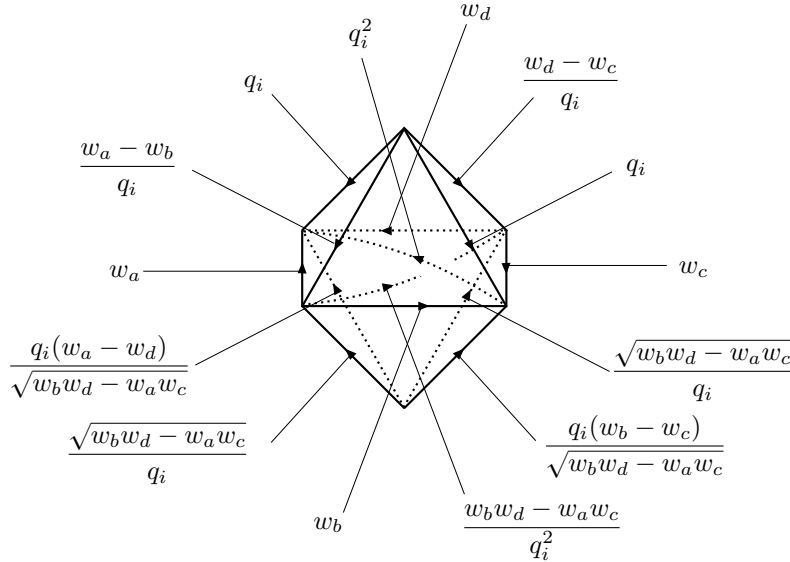


Figure 13: A Ptolemy assignment for a positive crossing.

The Ptolemy assignments given in Figures 13 and 14 satisfy the equation (3) for each ideal tetrahedron of o_i . It thus induces a natural $(\mathrm{SL}(2, \mathbb{C}), P)$ -cocycle $\mathcal{B}_i : \bar{\sigma}_i^1 \rightarrow \mathrm{SL}(2, \mathbb{C})$ (other than $\mathrm{PSL}(2, \mathbb{C})$). Using Lemma 3.3 in [21], short-edges parameters of \mathcal{B}_i for a

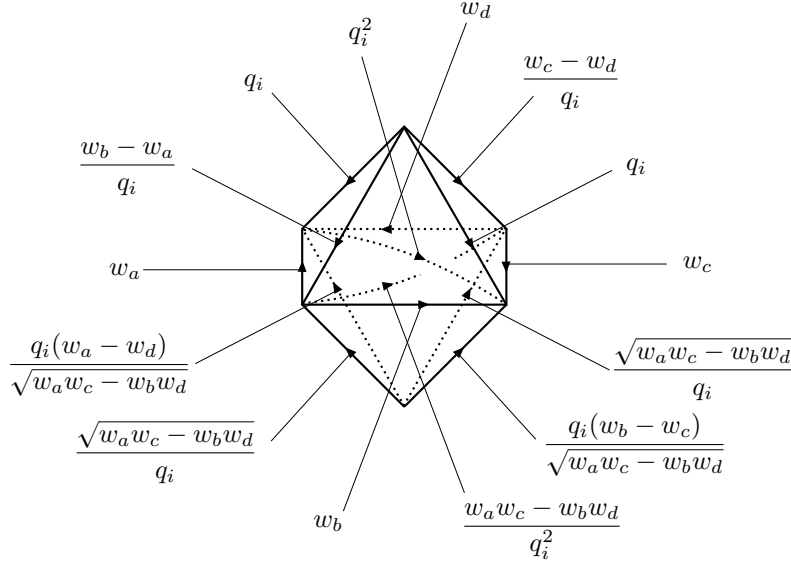


Figure 14: A Ptolemy assignment for a negative crossing.

positive crossing are computed as follows:

$$\begin{aligned}
\textcircled{a} &= \frac{w_d}{w_c - w_d} & \textcircled{b} &= \frac{w_a}{w_a - w_b} & \textcircled{c} &= \frac{w_b}{w_b - w_a} & \textcircled{d} &= \frac{w_c}{w_d - w_c} \\
\textcircled{e} &= \frac{w_b w_d - w_a w_c}{q_i^2 w_a (w_a - w_d)} & \textcircled{f} &= \frac{w_b w_d - w_a w_c}{q_i^2 w_d (w_d - w_a)} & \textcircled{g} &= \frac{w_d - w_c}{q_i^2 w_d} & \textcircled{h} &= \frac{w_b - w_a}{q_i^2 w_a} \\
\textcircled{i} &= \frac{q_i^2 (w_d - w_a)}{w_a (w_b w_d - w_a w_c)} & \textcircled{j} &= \frac{q_i^2 (w_b - w_c)}{w_b (w_b w_d - w_a w_c)} & \textcircled{k} &= \frac{q_i^2}{w_b (w_b - w_a)} & \textcircled{l} &= \frac{q_i^2}{w_a (w_a - w_b)} \\
\textcircled{m} &= \frac{w_b}{w_c - w_b} & \textcircled{n} &= \frac{w_c}{w_b - w_c} & \textcircled{o} &= \frac{w_d}{w_d - w_a} & \textcircled{p} &= \frac{w_a}{w_a - w_d} \\
\textcircled{q} &= \frac{w_b w_d - w_a w_c}{q_i^2 w_b (w_b - w_c)} & \textcircled{r} &= \frac{w_b w_d - w_a w_c}{q_i^2 w_c (w_c - w_b)} & \textcircled{s} &= \frac{w_d - w_c}{q_i^2 w_c} & \textcircled{t} &= \frac{w_b - w_a}{q_i^2 w_b} \\
\textcircled{u} &= \frac{q_i^2 (w_d - w_a)}{w_d (w_b w_d - w_a w_c)} & \textcircled{v} &= \frac{q_i^2 (w_b - w_c)}{w_c (w_b w_d - w_a w_c)} & \textcircled{w} &= \frac{q_i^2}{w_c (w_c - w_d)} & \textcircled{x} &= \frac{q_i^2}{w_d (w_d - w_c)}
\end{aligned} \tag{20}$$

for Figure 9. Short-edge parameters of \mathcal{B}_i for a negative crossing are the same as those for a positive crossing except that the sign of $\textcircled{a} \cdots, \textcircled{l}$ and $\textcircled{q} \cdots, \textcircled{x}$ should be changed.

3.2.2. Gluing the octahedra

As the ideal octahedra o_1, \dots, o_n glue their faces to form the manifold M , certain relations among the variables q_1, \dots, q_n are required to glue the natural cocycles \mathcal{B}_i 's compatibly. For convenience reasons, we define a η -value at a crossing by $\eta := w_b w_d - w_a w_c$ for Figure 12 (a) and $\eta := w_a w_c - w_b w_d$ for Figure 12 (b). Then one can check

that the relations among q_1, \dots, q_n consist of

$$\frac{q_i}{q_j} = \begin{cases} \frac{w_c - w_d}{\sqrt{\eta_j}} & \text{for Figure 15 (a)} \\ \frac{\sqrt{\eta_i}}{w_c - w_d} & \text{for Figure 15 (b)} \\ 1 & \text{for Figure 15 (c)} \\ \frac{\sqrt{\eta_i}}{\sqrt{\eta_j}} & \text{for Figure 15 (d)} \end{cases} \quad (21)$$

for each segment of D , where i and j are the indices of ideal octahedra placed at the crossing in the left and right of the segment, respectively.

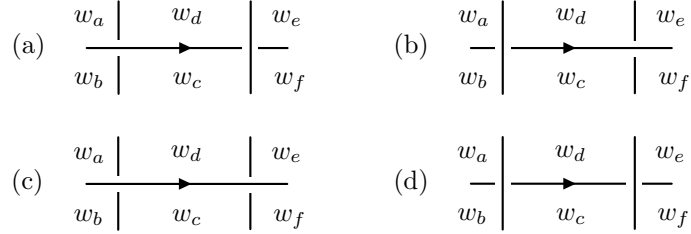


Figure 15: Region variables around a segment.

It turns out that it may not be possible to glue all \mathcal{B}_i 's compatibly (see Section 4). However, it is possible if we project them down to $\mathrm{PSL}(2, \mathbb{C})$ (see Proposition 3.7 below). Since the cocycle \mathcal{B}_i represents the same natural $(\mathrm{PSL}(2, \mathbb{C}), P)$ -cocycle for both q_i and $-q_i$, we may regard the variable q_i as an element of $\mathbb{C}^\times / \{\pm 1\}$.

Proposition 3.7. Regarding each q_i as an element of $\mathbb{C}^\times / \{\pm 1\}$, there exists a collection of q_1, \dots, q_n satisfying the equation (21) for every segment of D . Moreover, it is unique up to scaling.

Proof. As in the proof of Proposition 3.3, we consider a region, say R , of D and the equations (21) arising from the boundary segments of R . It suffices to check that the product of these equations results in the trivial equation up to sign.

Suppose that R is given as in Figure 16. Then relations among q_1, \dots, q_m arising from the segments lying in the boundary of R consist of

$$\frac{q_i}{q_{i+1}} = \frac{w_{2i+1} - w_0}{\sqrt{\eta_{i+1}}} \quad (22)$$

where $\eta_i = w_{2i-1}w_{2i} - w_0w_{2i}$ for $1 \leq i \leq m$. Here the index of q_i is taken in modulo m and that of w_i is taken in modulo $2m$. On the other hand, the equation (9) for the region R is given by

$$1 = \prod_{i=1}^m \frac{(w_{2i-1} - w_0)(w_{2i+1} - w_0)}{w_{2i-1}w_{2i+1} - w_0w_{2m}} = \prod_{i=1}^m \frac{(w_{2i+1} - w_0)^2}{\eta_i}.$$

Therefore, the product of the equations (22) for all $1 \leq i \leq n$ is trivial up to sign. If we change the orientation of a segment lying the boundary of R , the sign of two etas should be change. Therefore, the product of the equations (22) for all $1 \leq i \leq n$ does not depend on the orientation of segments. We proved the case when the boundary of R is alternating, but one can prove similarly for other cases. \square

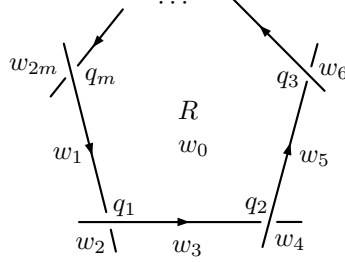


Figure 16: Region variables around a region.

Corollary 3.8. The natural cocycles $\mathcal{B}_i : \bar{o}_i^1 \rightarrow \text{PSL}(2, \mathbb{C})$ ($1 \leq i \leq n$) are well-glued so as to form a natural $(\text{PSL}(2, \mathbb{C}), P)$ -cocycle $\mathcal{B} : \bar{M}^1 \rightarrow \text{PSL}(2, \mathbb{C})$ on the manifold M .

In particular, we obtain a Ptolemy assignment $c : M^1 \rightarrow \mathbb{C}^\times$ after some sign-choices. Due to Proposition 2.13 such c is a point of $P^\sigma(\mathcal{F}_5)$ for some $\sigma \in Z^2(\widehat{M}; \{\pm 1\})$ whose class is the obstruction class of the holonomy representation ρ . We shall analyze this class in Section 4.

4. Obstruction classes

Let K be a knot in S^3 with a fixed diagram D and let $M = S^3 \setminus (K \cup \{p, q\})$ where $p \neq q \in S^3$ are two points not in K . Due to Poincaré-Lefschetz duality, we have

$$H^2(\bar{M}, \partial\bar{M}; \{\pm 1\}) \simeq H_1(\bar{M}; \{\pm 1\}) \simeq \{\pm 1\}.$$

Thus the obstruction class of a $(\text{PSL}(2, \mathbb{C}), P)$ -representation $\pi_1(M) \rightarrow \text{PSL}(2, \mathbb{C})$ can be viewed as an element of $\{\pm 1\}$. Main aim of this section is to present a diagrammatic formula for computing the obstruction class.

We enumerate the crossings of D by c_i ($1 \leq i \leq n$) and define $\sigma(c_i) \in \mathbb{C}^\times$ by

$$\sigma(c_i) := \frac{z_a}{z_c}$$

when segment variables around the crossing c_i are given as in either Figure 6 (a) or (b). Similarly, when region variables around c_i are given as in either Figure 12 (a) or (b) we let

$$\sigma(c_i) := \frac{w_a - w_d}{w_b - w_c}.$$

Then the obstruction class viewed as an element of $\{\pm 1\}$ is computed as follows.

Theorem 4.1. For a collection of segment (resp., region) variables satisfying the gluing equations of \mathcal{F}_4 (resp., \mathcal{F}_5), the obstruction class of the holonomy representation $\rho : \pi_1(M) \rightarrow \mathrm{PSL}(2, \mathbb{C})$ is given by

$$\prod_{i=1}^n \sigma(c_i) \in \{\pm 1\} \simeq H^2(\overline{M}, \partial \overline{M}; \{\pm 1\}).$$

Remark 4.2. It is known that the geometric representation of a hyperbolic knot has the non-trivial obstruction class (see e.g. [1], [11, §3.2]). Thus a simple corollary follows: if $\prod \sigma(c_i) \neq -1$, then the holonomy representation is not geometric.

4.1. Proof of Theorem 4.1

For a given collection of segment or region variables let $\mathcal{B} : \overline{M}^1 \rightarrow \mathrm{PSL}(2, \mathbb{C})$ be a natural cocycle given in Corollary 3.5 or 3.8. Recall that the long-edge parameters $c : M^1 \rightarrow \mathbb{C}^\times / \{\pm 1\}$ have sign-ambiguity as we are working on $\mathrm{PSL}(2, \mathbb{C})$.

The manifold M has two ideal vertices p and q whose link are spheres. One of them lies over the diagram while the other one lies below. We may assume that the vertex p lies above the diagram. The edges of M joining p with the ideal vertex corresponding to the knot K are called *over-edges* in [10] and they are in one-to-one correspondence with the (over-)arcs of D . We enumerate the arcs by a_i ($1 \leq i \leq n$) along the diagram and denote by v_i the over-edge corresponding to a_i . Also, we may assume that a crossing c_i lies between a_{i-1} and a_i (see Figure 17). Here the index is taken in modulo n .

At each crossing c_i , both v_{i-1} and v_i appear as lower hypotenuses of the ideal octahedron o_i as in Figure 17. The Ptolemy assignments on o_i given in Section 3 (Figures 8, 13, 14) show that

$$\frac{c(v_{i-1})}{c(v_i)} = \sigma(c_i)$$

up to sign. It thus follows that

$$\prod_{i=1}^n \sigma(c_i) = \prod_{i=1}^n \frac{c(v_{i-1})}{c(v_i)} = \pm 1. \quad (23)$$

Remark 4.3. The equation (23) gives a polynomial equality $\prod_{i=1}^n \sigma(c_i)^2 = 1$ in region or segment variables. The authors do not know whether this equality can be directly derived from the gluing equations of \mathcal{F}_4 or \mathcal{F}_5 .

Lemma 4.4. If $\prod \sigma(c_i) = 1$, then \mathcal{B} lifts to a natural $(\mathrm{SL}(2, \mathbb{C}), P)$ -cocycle.

Proof. Recall Proposition 3.3 (or 3.7) that the natural cocycle \mathcal{B} is induced from a collection of the variables $p_i \in \mathbb{C}^\times / \{\pm 1\}$ (or q_i) satisfying certain relations. Even though each p_i and q_i is defined up to sign, the short-edge parameters are well-defined without sign-ambiguity (see the equation (15) and (20)). This allows us to define an $\mathrm{SL}(2, \mathbb{C})$ -lifting $\tilde{\mathcal{B}}(e) \in \mathrm{SL}(2, \mathbb{C})$ of $\mathcal{B}(e)$ for each short-edge e of \overline{M} . Remark that $\tilde{\mathcal{B}}(e) \in P$ for all short-edges e . In particular, $\tilde{\mathcal{B}}$ satisfies cocycle condition for all triangular faces of \overline{M} . Therefore, it is enough to show that there exists an $\mathrm{SL}(2, \mathbb{C})$ -lifting $\tilde{\mathcal{B}}(e)$ of $\mathcal{B}(e)$ for each long-edge e of \overline{M} so that $\tilde{\mathcal{B}} : \overline{M}^1 \rightarrow \mathrm{SL}(2, \mathbb{C})$ satisfies cocycle condition for all hexagonal faces of \overline{M} . We denote by $\tilde{c} : M^1 \rightarrow \mathbb{C}^\times$ the long-edge parameters of $\tilde{\mathcal{B}}$.

For each long-edge e of \overline{M} joining the ideal vertices q and p , the long-edge parameter $c(e)$ is an even function in the variable p_i (or q_i). See Figures 8, 13 and 14. Thus $c(e)$ is well-defined without sign-ambiguity. In particular, letting $\tilde{c}(e) := c(e)$, a lifting $\tilde{\mathcal{B}}(e)$ of $\mathcal{B}(e)$ is determined.

We then consider an over-edge v_i ($1 \leq i \leq n$). Recall that the corresponding arc a_i of D runs from the crossings c_i to c_{i+1} . At each crossing in between c_i and c_{i+1} , the over-edge v_i appears twice as upper-hypotenuses. We enumerate the upper-hypotenuses at these intermediate crossings other than v_i by u_1, \dots, u_m as in Figure 17. For each u_j ($1 \leq j \leq m$) there are two hexagonal faces, say F_1 and F_2 , of \overline{M} containing both v_i and u_j (we have indicated F_1 and F_2 for u_2 in Figure 17). The boundary of $F_1 \cup F_2$ consists of short-edges and long-edges joining q and p ; both v_i and u_j are canceled out when we glue F_1 and F_2 . In particular, the $\tilde{\mathcal{B}}$ -matrices for the boundary edges of $F_1 \cup F_2$ are already chosen and by construction $\tilde{\mathcal{B}}$ satisfies cocycle condition for $F_1 \cup F_2$. This implies that whenever we choose a lifting $\tilde{\mathcal{B}}(v_i)$, there is a unique lifting $\tilde{\mathcal{B}}(u_j)$ so that $\tilde{\mathcal{B}}$ satisfies cocycle condition for both F_1 and F_2 . Applying the same argument for u_m and v_{i+1} (see the lower-hypotenuses at c_{i+1}), one can conclude that a lifting $\tilde{\mathcal{B}}(u_m)$ uniquely determines $\tilde{\mathcal{B}}(v_{i+1})$ so as to $\tilde{\mathcal{B}}$ satisfy cocycle condition for each hexagonal face containing both u_m and v_{i+1} .

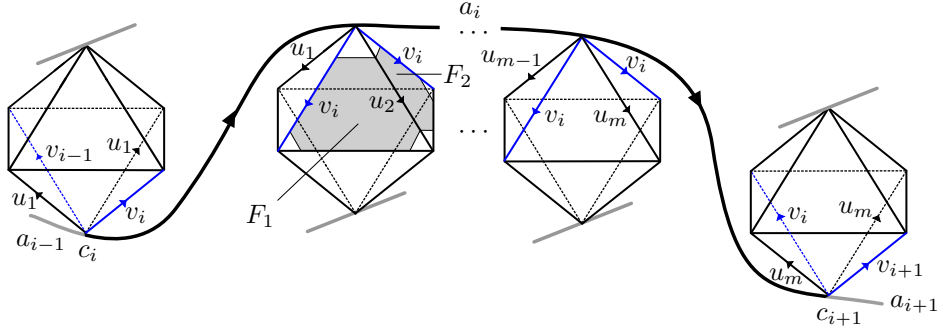


Figure 17: An over-arc: faces F_1 and F_2 for u_2 .

We now fix a crossing c_1 as a starting point and choose a lifting $\tilde{\mathcal{B}}(v_1) \in \mathrm{SL}(2, \mathbb{C})$. The argument in the previous paragraph tells us that along the diagram, $\tilde{\mathcal{B}}(v_1)$ uniquely determines liftings $\tilde{\mathcal{B}}(e)$ for all hypotenuses e of the ideal octahedra o_1, \dots, o_n so that $\tilde{\mathcal{B}}$ satisfies cocycle condition for all boundary faces of $\overline{o_1}, \dots, \overline{o_n}$, except for lower hexagonal faces of $\overline{o_1}$. On the other hand, the uniqueness of such determination gives that

$$\frac{\tilde{c}(v_i)}{\tilde{c}(v_{i+1})} = \sigma(c_{i+1}) \quad (24)$$

for $1 \leq i \leq n-1$ (see Figures 8, 13, 14). Since we have $\prod_{i=1}^n \sigma(c_i) = 1$, the equation (24) also hold for $i = n$. This implies that $\tilde{\mathcal{B}}$ satisfies cocycle condition also for lower hexagonal faces of $\overline{o_1}$.

We so far have chosen $\tilde{\mathcal{B}}(e)$ for the boundary edges e of $\overline{o_1}, \dots, \overline{o_n}$ to satisfy cocycle condition for all boundary faces of $\overline{o_1}, \dots, \overline{o_n}$. Therefore, there exists a lifting $\tilde{\mathcal{B}}(e)$ for the long-edges e created to subdivide o_1, \dots, o_n into ideal tetrahedra so that $\tilde{\mathcal{B}} : \overline{M}^1 \rightarrow$

$\mathrm{SL}(2, \mathbb{C})$ satisfies cocycle condition for all faces of \overline{M} . This completes the construction of a natural $(\mathrm{SL}(2, \mathbb{C}), P)$ -cocycle $\tilde{\mathcal{B}}$ which is a lifting of \mathcal{B} . \square

Lemma 4.4 implies that if $\prod \sigma(c_i) = 1$, then ρ admits a $(\mathrm{SL}(2, \mathbb{C}), P)$ -lifting $\tilde{\rho} : \pi_1(M) \rightarrow \mathrm{SL}(2, \mathbb{C})$. In particular, we have $\mathrm{tr}(\tilde{\rho}(\lambda)) = 2$ for a (canonical) longitude λ . It follows from Proposition 2.2 in [5] that the obstruction class of ρ is 1. For convenience of the reader, we recall Proposition 2.2 in [5] here:

Proposition 4.5 ([5]). The obstruction class of a $(\mathrm{PSL}(2, \mathbb{C}), P)$ -representation $\rho : \pi_1(M) \rightarrow \mathrm{PSL}(2, \mathbb{C})$ viewed as an element of $\{\pm 1\}$ coincides with half of $\mathrm{tr}(\tilde{\rho}(\lambda))$ where $\tilde{\rho}$ is an $\mathrm{SL}(2, \mathbb{C})$ -lifting of ρ and λ is a canonical longitude of the knot K .

Lemma 4.6. If $\prod \sigma(c_i) = -1$, ρ admits an $\mathrm{SL}(2, \mathbb{C})$ -lifting $\tilde{\rho}$ such that $\mathrm{tr}(\tilde{\rho}(\lambda)) = -2$.

Proof. We proceed the same construction for an $\mathrm{SL}(2, \mathbb{C})$ -lifting $\tilde{\mathcal{B}}$ of \mathcal{B} as in the proof of Lemma 4.4. Then one can determine $\tilde{\mathcal{B}}(e)$ for all boundary edges e of $\overline{o}_1, \dots, \overline{o}_n$ so that $\tilde{\mathcal{B}}$ satisfies cocycle condition for all boundary faces of $\overline{o}_1, \dots, \overline{o}_n$, except lower hexagonal faces of \overline{o}_1 . More precisely, since we have $\prod \sigma(c_i) = -1$, $\tilde{\mathcal{B}}$ does not satisfy cocycle condition for two hexagonal faces F_1 and F_2 containing both v_n and u , where u is the lower-hypotenuse of o_1 other than v_1 and v_n (see Figure 18).

To make $\tilde{\mathcal{B}}$ be a cocycle, we have to change the sign of $\tilde{\mathcal{B}}(e_i)$ for the short-edge e_i of F_i ($i = 1, 2$) near to the bottom vertex of o_1 . If we are working on \mathcal{J}_4 , we also change the sign of $\tilde{\mathcal{B}}(e_3)$ for the short-edge e_3 described as in Figure 18. Then one can easily check that $\tilde{\mathcal{B}}$ now satisfies cocycle condition for all boundary faces of $\overline{o}_1, \dots, \overline{o}_n$. As in the proof of Lemma 4.4, we finally choose $\tilde{\mathcal{B}}(e)$ for the long-edges e created to subdivide o_1, \dots, o_n into ideal tetrahedra so that $\tilde{\mathcal{B}} : \overline{M}^1 \rightarrow \mathrm{SL}(2, \mathbb{C})$ satisfies cocycle condition for all faces of \overline{M} . We stress that $\tilde{\mathcal{B}}$ is a cocycle but not a natural $(\mathrm{SL}(2, \mathbb{C}), P)$ -cocycle ($\tilde{\mathcal{B}}(e_i) \notin P$).

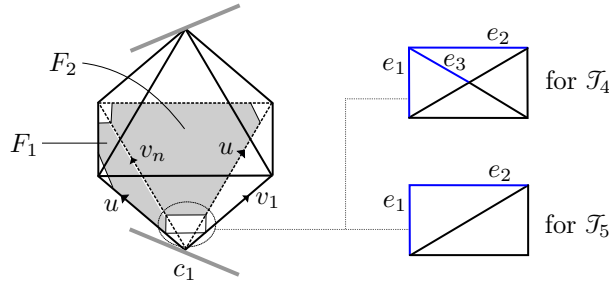


Figure 18: Sign-change for the short-edges.

Let $\tilde{\rho} : \pi_1(M) \rightarrow \mathrm{SL}(2, \mathbb{C})$ be a representation induced from the cocycle $\tilde{\mathcal{B}}$. For a meridian μ of K , there is an edge-path of \overline{M} which is homotopic to μ and not passes through the short-edges e_i 's. It thus follows that $\mathrm{tr}(\tilde{\rho}(\mu)) = 2$. Similarly, for a (canonical) longitude λ , there is an edge-path of \overline{M} which is homotopic to λ and passes through the short-edges e_i 's exactly once. We thus obtain $\mathrm{tr}(\tilde{\rho}(\lambda)) = -2$. \square

Theorem 4.1 then follows from Lemmas 4.4 and 4.6 with Proposition 4.5.

Example 4.7. Let us consider the figure-eight knot with a diagram given as in Figure 19. It is proved in [10] that segment variables

$$(z_1, \dots, z_8) = \left(1 + i, i(1 + \sqrt{3}), \frac{-1 + i\sqrt{3}}{-1 + \sqrt{3}}, 2i, -1 + i, i, \frac{1 + i\sqrt{3}}{-1 + \sqrt{3}}, -\frac{2i}{-1 + \sqrt{3}} \right)$$

satisfy the gluing equations of \mathcal{T}_4 (these are obtained by putting $p = 1 + i$, $q = 1 - i$, $r = 1$ in Example 4.6 of [10]). Applying Theorem 4.1, the obstruction class of the holonomy representation is given by

$$\prod_{i=1}^4 \sigma(c_i) = \frac{1 + i}{i(1 + \sqrt{3})} \cdot \frac{-1 + i\sqrt{3}}{2i(-1 + \sqrt{3})} \cdot \frac{-1 + i}{i} \cdot \frac{1 + i\sqrt{3}}{-2i} = -1.$$

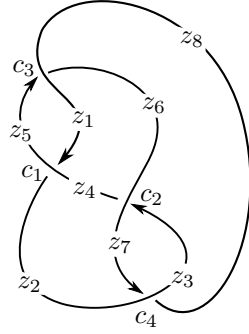


Figure 19: The figure-eight knot.

Example 4.8. Let us consider the trefoil knot with a diagram given as in Figure 20 (left). It is proved in [2] that region variables $(w_1, \dots, w_6) = (5, 3, 7, 2, 1, 8)$ satisfy the gluing equations of \mathcal{T}_5 . Applying Theorem 4.1, the obstruction class of the holonomy representation is given by

$$\prod_{i=1}^4 \sigma(c_i) = -2 \cdot \frac{1}{3} \cdot 1 \cdot \frac{3}{2} = -1$$

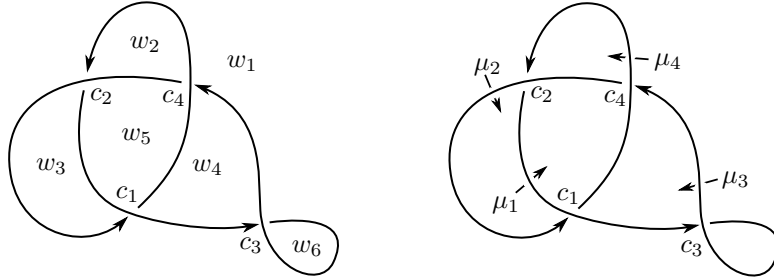


Figure 20: The trefoil knot with a kink.

Remark 4.9. As the diagram in Figure 20 has a kink, the ideal triangulation \mathcal{T}_4 has a degenerate edge. It implies that the gluing equations of \mathcal{T}_4 has no solution (see [14]). In particular, one can not handle the diagram with segment variables. Meanwhile, it is proved by Cho [2] that the gluing equation variety of \mathcal{T}_5 produce all $(\mathrm{PSL}(2, \mathbb{C}), P)$ -representations except the trivial one for any knot diagram.

5. Holonomy representations

Let K be a knot in S^3 with a fixed diagram D and let $M = S^3 \setminus (K \cup \{p, q\})$ where $p \neq q \in S^3$ are two points not in K . We enumerate the crossings of D by c_i ($1 \leq i \leq n$). For notational convenience, we assume that the index of the crossings c_i increases whenever we under-pass the crossing along the diagram (as in Figure 17).

Throughout the section, we fix a collection of segment (resp., region) variables satisfying the gluing equations of \mathcal{T}_4 (resp., \mathcal{T}_5) and let $\rho : \pi_1(M) \rightarrow \mathrm{PSL}(2, \mathbb{C})$ be the holonomy representation. As we have computed a natural cocycle $\mathcal{B} : \overline{M}^1 \rightarrow \mathrm{PSL}(2, \mathbb{C})$ in Section 3, an explicit computation for ρ can be simply carried out: recall that for $\gamma \in \pi_1(M)$, $\rho(\gamma)$ is given by the product of \mathcal{B} -matrices along an edge-path of \overline{M} homotopic to γ (see Proposition 2.9). We devote this section to present some explicit computations. We note that similar computations can be found in [10].

5.1. The cusp shape

For each crossing c_i we define $\lambda(c_i) \in \mathbb{C}^\times$ by

$$\lambda(c_i) := \frac{z_b z_d (z_c - z_a)}{z_a z_c (z_b - z_d)}$$

when segment variables around c_i are given as in either Figure 6 (a) or (b). Similarly, when region variables around c_i are given as in either Figure 12 (a) or (b), we let

$$\lambda(c_i) := \frac{w_a w_c - w_b w_d}{(w_a - w_d)(w_c - w_b)}.$$

Theorem 5.1. Let μ be a meridian of K and λ_D be a longitude with the blackboard framing with respect to D . Then we have

$$\rho(\mu) = \begin{pmatrix} 1 & 1 \\ 0 & 1 \end{pmatrix}, \quad \rho(\lambda_D) = \begin{pmatrix} 1 & \sum_{i=1}^n \lambda(c_i) \\ 0 & 1 \end{pmatrix} \quad (25)$$

up to conjugation. Therefore, the cusp shape of ρ is given by

$$\sum_{i=1}^n \lambda(c_i) - w(D)$$

where $w(D)$ denotes the writhe of D .

Proof. For each crossing c_i we denote by d_i the diagonal of the bottom quadrilateral of \bar{o}_i parallel to D . In Figure 9 the diagonal d_i is homotopic to the composition of two short-edges $\textcircled{\text{P}} * \textcircled{\text{m}}$. From the equations (15) and (20) one can check that the sum of these short-edge parameters is $\lambda(c_i)$. The $\rho(\lambda_D)$ -part of the equation (25) follows from the fact that the composition $d_1 * \dots * d_n$ is homotopic to the blackboard framed longitude λ_D . In a similar manner, the meridian μ is homotopic to the composition of two short-edges $\textcircled{\text{P}} * \textcircled{\text{O}}$ and the sum of these short-edge parameters is 1. This proves the equation (25).

The second part of the theorem directly follows from the fact that λ_D winds the knot $w(D)$ times. \square

Remark 5.2. In the proof of Theorem 5.1 one can use the diagonal of the top (instead of bottom) quadrilateral of \bar{o}_i parallel to D . A similar argument shows that the cusp shape is alternatively given by

$$\sum_{i=1}^n \lambda'(c_i) - w(D)$$

where $\lambda'(c_i)$ is given by

$$\lambda'(c_i) = \frac{z_b - z_d}{z_c - z_a} \quad \text{for Figure 6 (a) and (b)}$$

or

$$\lambda'(c_i) = \frac{w_a w_c - w_b w_d}{(w_a - w_b)(w_c - w_d)} \quad \text{for Figure 12 (a) and (b)}.$$

Example 5.3. We continue Example 4.7 of the figure-eight knot. Applying Theorem 5.1, the cusp shape of the holonomy representation ρ is given by

$$\sum_{i=1}^4 \lambda(c_i) - w(D) = \left(1 + i(\sqrt{3} - 2) + \frac{1 + i\sqrt{3}}{2 + 2\sqrt{3}} + \frac{1 + i}{\sqrt{3} + i} + \frac{2 + \sqrt{3} + i}{-2 + \sqrt{3} - i} \right) - 0 = 2\sqrt{3}i.$$

Example 5.4. We continue Example 4.8 of the trefoil knot. Applying Theorem 5.1, the cusp shape of the holonomy representation ρ is given by

$$\sum_{i=1}^4 \lambda(c_i) - w(D) = \left(-\frac{9}{2} + \frac{4}{3} - 1 + \frac{1}{6} \right) - 2 = -6.$$

5.2. Wirtinger generators

We denote by a_i the arc of D running from c_i to c_{i+1} (as in Figure 17) and denote by μ_i the Wirtinger generator winding the over-arc of a crossing c_i respecting the orientation. See, for instance, Figure 20 (right). Let e_i be the crossing-sign of c_i .

When segment variables around a crossing c_i are given as in either Figure 6 (a) or (b), we define $M(c_i) \in \text{PSL}(2, \mathbb{C})$ by

$$M(c_i) := \begin{pmatrix} \frac{z_a}{z_c} & \frac{z_b z_d (z_c - z_a)}{z_c^2 (z_b - z_d)} \\ \frac{(z_a - z_c)(z_b - z_d)}{z_b z_d} & 2 - \frac{z_a}{z_c} \end{pmatrix}.$$

Similarly, when region variables around c_i are given as in either Figure 12 (a) or (b), we define $M(c_i) \in \text{PSL}(2, \mathbb{C})$ by

$$M(c_i) := \begin{pmatrix} \frac{w_a - w_d}{w_b - w_c} & \frac{w_b w_d - w_a w_c}{(w_b - w_c)^2} \\ \frac{(w_a - w_b + w_c - w_d)^2}{w_a w_c - w_b w_d} & 2 - \frac{w_a - w_d}{w_b - w_c} \end{pmatrix}.$$

Then the ρ -image of the Wirtinger generators is inductively computed as follows.

Theorem 5.5. For $1 \leq i \leq n$ we have

$$\rho(\mu_i^{e_i}) = \rho(\mu_1^{e_1} \cdots \mu_{i-1}^{e_{i-1}})^{-1} \begin{pmatrix} 1 & \sum_{j=1}^i \lambda(c_j) \\ 0 & 1 \end{pmatrix} M(c_i) \begin{pmatrix} 1 & \sum_{j=1}^i \lambda(c_j) \\ 0 & 1 \end{pmatrix}^{-1} \rho(\mu_1^{e_1} \cdots \mu_{i-1}^{e_{i-1}})$$

Proof. As in the proof of Theorem 5.1 we denote by d_j the diagonal of the bottom quadrilateral of $\bar{\sigma}_j$ parallel to the diagram D . Let A_1 be the composition $d_1 * \cdots * d_i$, a path from o_1 to o_i following D , and let $\underline{\mu}_i$ be a loop that (1) first follows the path A_1 ; (2) then winds the over-arc of the crossing c_i respecting the orientation; (3) then returns through (the reverse of) A_1 . See Figure 21.

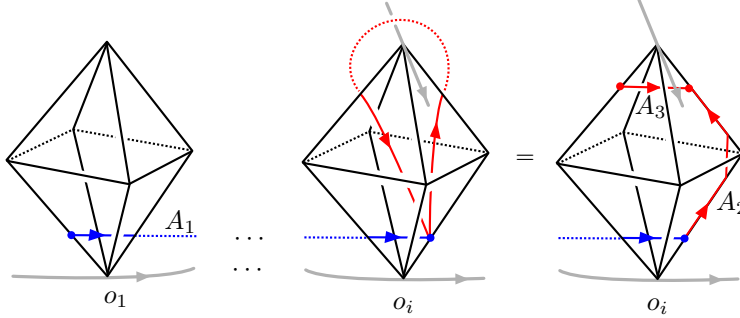


Figure 21: The loop $\underline{\mu}_i$.

As we computed in the proof of Theorem 5.1, the sum of short-edge parameters along the path A_1 is given by $\sum_{j=1}^i \lambda(c_j)$. For the second part (2) of the loop $\underline{\mu}_i$, using the parameters given in Section 3.2, the product of \mathcal{B} -matrices along the edge-path $A_2 * A_3 * A_2^{-1}$ depicted in Figure 21 is in fact the matrix $M(c_i)^{e_i}$. We thus obtain

$$\rho(\underline{\mu}_i) = \begin{pmatrix} 1 & \sum_{j=1}^i \lambda(c_j) \\ 0 & 1 \end{pmatrix} M(c_i)^{e_i} \begin{pmatrix} 1 & \sum_{j=1}^i \lambda(c_j) \\ 0 & 1 \end{pmatrix}^{-1}.$$

The theorem then follows from Lemma 5.1 in [10], which says that the loop $\underline{\mu}_i$ is homotopic to $(\mu_1^{e_1} \cdots \mu_{i-1}^{e_{i-1}}) \mu_i (\mu_1^{e_1} \cdots \mu_{i-1}^{e_{i-1}})^{-1}$. \square

Example 5.6. We continue Example 4.8 of the trefoil knot. Recall that we have $(e_1, e_2, e_3, e_4) = (1, 1, -1, 1)$ and $(\lambda(c_1), \lambda(c_2), \lambda(c_3), \lambda(c_4)) = (-\frac{9}{2}, \frac{4}{3}, -1, \frac{1}{6})$ (see Example 5.4). A simple computation gives

$$M(c_1) = \begin{pmatrix} -2 & 9 \\ -1 & 4 \end{pmatrix}, M(c_2) = \begin{pmatrix} \frac{1}{3} & \frac{4}{9} \\ -1 & \frac{5}{3} \end{pmatrix}, M(c_3) = \begin{pmatrix} 1 & -1 \\ 0 & 1 \end{pmatrix}, M(c_4) = \begin{pmatrix} \frac{3}{2} & \frac{1}{4} \\ -1 & \frac{1}{2} \end{pmatrix}.$$

Applying Theorem 5.5, the ρ -image of the Wirtinger generators is computed as follow (see Figure 20 (right)):

- $\rho(\mu_1^{e_1}) = \begin{pmatrix} 1 & -\frac{9}{2} \\ 0 & 1 \end{pmatrix} M(c_1) \begin{pmatrix} 1 & -\frac{9}{2} \\ 0 & 1 \end{pmatrix}^{-1} = \begin{pmatrix} \frac{5}{2} & \frac{9}{4} \\ -1 & -\frac{1}{2} \end{pmatrix};$
- $\rho(\mu_2^{e_2}) = \rho(\mu_1^{e_1})^{-1} \begin{pmatrix} 1 & -\frac{19}{6} \\ 0 & 1 \end{pmatrix} M(c_2) \begin{pmatrix} 1 & -\frac{19}{6} \\ 0 & 1 \end{pmatrix}^{-1} \rho(\mu_1^{e_1}) = \begin{pmatrix} 1 & 1 \\ 0 & 1 \end{pmatrix};$
- $\rho(\mu_3^{e_3}) = \rho(\mu_1^{e_1} \mu_2^{e_2})^{-1} \begin{pmatrix} 1 & -\frac{25}{6} \\ 0 & 1 \end{pmatrix} M(c_3) \begin{pmatrix} 1 & -\frac{25}{6} \\ 0 & 1 \end{pmatrix}^{-1} \rho(\mu_1^{e_1} \mu_2^{e_2}) = \begin{pmatrix} -\frac{1}{2} & -\frac{9}{4} \\ 1 & \frac{5}{2} \end{pmatrix};$
- $\rho(\mu_4^{e_4}) = \rho(\mu_1^{e_1} \mu_2^{e_2} \mu_3^{e_3})^{-1} \begin{pmatrix} 1 & -4 \\ 0 & 1 \end{pmatrix} M(c_4) \begin{pmatrix} 1 & -4 \\ 0 & 1 \end{pmatrix}^{-1} \rho(\mu_1^{e_1} \mu_2^{e_2} \mu_3^{e_3}) = \begin{pmatrix} \frac{3}{2} & \frac{1}{4} \\ -1 & \frac{1}{2} \end{pmatrix}.$

5.3. The complex volume

For a $(\mathrm{PSL}(2, \mathbb{C}), P)$ -representation ρ , the *complex volume* is defined by

$$\mathrm{Vol}_{\mathbb{C}}(\rho) := \mathrm{Vol}(\rho) + i\mathrm{CS}(\rho) \in \mathbb{C}/i\pi^2\mathbb{Z}$$

where Vol and CS denote the volume and Chern-Simons invariant, respectively. We refer to [9] for details. In [4] and [3], they presented formulas for computing the complex volume in terms of segment and region variables, respectively. For convenience of the reader, we here recall these formulas. Note that as the diagram D has n crossings, there are $2n$ segments and $n + 2$ regions.

We first consider the case of segment variables. For each crossing c_i given as in either Figure 6 (a) or (b), we associate a function

$$\mathrm{Li}_2\left(\frac{z_c}{z_b}\right) - \mathrm{Li}_2\left(\frac{z_c}{z_d}\right) + \mathrm{Li}_2\left(\frac{z_a}{z_d}\right) - \mathrm{Li}_2\left(\frac{z_a}{z_b}\right)$$

to the crossing where Li_2 denotes the dilogarithm function (see, for instance, [20]). We then define the *potential function* $V(z_1, \dots, z_{2n})$ of the diagram D by the sum of such functions over the crossings. In a similar manner, for the case of region variables we associate a function

$$-\mathrm{Li}_2\left(\frac{w_d}{w_a}\right) - \mathrm{Li}_2\left(\frac{w_d}{w_c}\right) + \mathrm{Li}_2\left(\frac{w_b w_d}{w_a w_c}\right) + \mathrm{Li}_2\left(\frac{w_a}{w_b}\right) + \mathrm{Li}_2\left(\frac{w_c}{w_b}\right) - \frac{\pi^2}{6} + \log \frac{w_a}{w_b} \log \frac{w_c}{w_b}$$

to a crossing as in Figure 12 (a) and

$$\operatorname{Li}_2\left(\frac{w_a}{w_b}\right) + \operatorname{Li}_2\left(\frac{w_a}{w_d}\right) - \operatorname{Li}_2\left(\frac{w_a w_c}{w_b w_d}\right) - \operatorname{Li}_2\left(\frac{w_b}{w_c}\right) - \operatorname{Li}_2\left(\frac{w_d}{w_c}\right) + \frac{\pi^2}{6} - \log \frac{w_b}{w_c} \log \frac{w_d}{w_c}$$

to a crossing as in Figure 12 (b). We then define the potential function $W(w_1, \dots, w_{n+2})$ of the diagram D by the sum of such functions over the crossings. Then the complex volume of the holonomy representation ρ is computed as follows.

Theorem 5.7 ([3]). The complex volume of the holonomy representation ρ is given by

$$i\operatorname{Vol}_{\mathbb{C}}(\rho) \equiv V_0(z_1, \dots, z_{2n}) \pmod{\pi^2}$$

where the function V_0 is defined by

$$V_0(z_1, \dots, z_{2n}) := V(z_1, \dots, z_{2n}) - \sum_{i=1}^{2n} \left(z_i \frac{\partial V}{\partial z_i} \right) \log z_i.$$

Theorem 5.8 ([4]). The complex volume of the holonomy representation ρ is given by

$$i\operatorname{Vol}_{\mathbb{C}}(\rho) \equiv W_0(w_1, \dots, w_{n+2}) \pmod{\pi^2}$$

where the function W_0 is defined by

$$W_0(w_1, \dots, w_{n+2}) := W(w_1, \dots, w_{n+2}) - \sum_{i=1}^{n+2} \left(w_i \frac{\partial W}{\partial w_i} \right) \log w_i.$$

References

- [1] D. Calegari. Real places and torus bundles. *Geometriae Dedicata*, 118(1):209–227, 2006.
- [2] J. Cho. Optimistic limit of the colored Jones polynomial and the existence of a solution. *Proceedings of the American Mathematical Society*, 144(4):1803–1814, 2016.
- [3] J. Cho, H. Kim, and S. Kim. Optimistic limits of Kashaev invariants and complex volumes of hyperbolic links. *Journal of Knot Theory and Its Ramifications*, 23(09):1450049, 2014.
- [4] J. Cho and J. Murakami. Optimistic limits of the colored Jones polynomials. *J. Korean Math. Soc.*, 50(3):641–693, 2013.
- [5] J. Cho, S. Yoon, and C. K. Zickert. On the Hikami-Inoue conjecture. *preprint arXiv:1805.11841, to appear in Algebraic Geometry and Topology*, 2018.
- [6] V. Fock and A. Goncharov. Moduli spaces of local systems and higher Teichmüller theory. *Publications Mathématiques de l’IHÉS*, 103:1–211, 2006.
- [7] S. Garoufalidis, M. Goerner, and C. K. Zickert. Gluing equations for $\operatorname{PGL}(n, \mathbb{C})$ -representations of 3-manifolds. *Algebraic & Geometric Topology*, 15(1):565–622, 2015.
- [8] S. Garoufalidis, M. Goerner, and C. K. Zickert. The Ptolemy field of 3-manifold representations. *Algebraic & Geometric Topology*, 15(1):371–397, 2015.
- [9] S. Garoufalidis, D. P. Thurston, and C. K. Zickert. The complex volume of $\operatorname{SL}(n, \mathbb{C})$ -representations of 3-manifolds. *Duke Mathematical Journal*, 164(11):2099–2160, 2015.
- [10] H. Kim, S. Kim, and S. Yoon. Octahedral developing of knot complement I: pseudo-hyperbolic structure. *Geometriae Dedicata*, 197(1):123–172, 2018.
- [11] P. Menal-Ferrer and J. Porti. Twisted cohomology for hyperbolic three manifolds. *Osaka Journal of Mathematics*, 49(3):741–769, 2012.
- [12] W. Neumann and A. Tsvietkova. Intercusp geodesics and the invariant trace field of hyperbolic 3-manifolds. *Proceedings of the American Mathematical Society*, 144(2):887–896, 2016.

- [13] W. D. Neumann and D. Zagier. Volumes of hyperbolic three-manifolds. *Topology*, 24(3):307–332, 1985.
- [14] H. Segerman and S. Tillmann. Pseudo-developing maps for ideal triangulations I: essential edges and generalised hyperbolic gluing equations. *Topology and geometry in dimension three*, 560:85–102, 2011.
- [15] M. Thistlethwaite and A. Tsvietkova. An alternative approach to hyperbolic structures on link complements. *Algebraic & Geometric Topology*, 14(3):1307–1337, 2014.
- [16] D. Thurston. Hyperbolic volume and the Jones polynomial. *handwritten note in Grenoble summer school*, 1999.
- [17] W. P. Thurston. *The geometry and topology of three-manifolds*. Princeton University, NJ:Princeton, 1979.
- [18] J. Weeks. Computation of hyperbolic structures in knot theory. In *Handbook of knot theory*, pages 461–480. Elsevier, 2005.
- [19] Y. Yokota. On the volume conjecture for hyperbolic knots. *arXiv:math/0009165*, 2000.
- [20] D. Zagier. The dilogarithm function. In *Frontiers in number theory, physics, and geometry II*, pages 3–65. Springer, 2007.
- [21] C. K. Zickert. The volume and Chern-Simons invariant of a representation. *Duke Mathematical Journal*, 150(3):489–532, 2009.